

Sample-Efficient Linear Representation Learning from Non-IID Non-Isotropic Data

Thomas T. Zhang^{1*}, Leonardo F. Toso², James Anderson², Nikolai Matni¹

¹ Department of Electrical and Systems Engineering, University of Pennsylvania

² Department of Electrical Engineering, Columbia University

Abstract

A powerful concept behind much of the recent progress in machine learning is the extraction of common features across data from heterogeneous sources or tasks. Intuitively, using all of one’s data to learn a common representation function benefits both computational effort and statistical generalization by leaving a smaller number of parameters to fine-tune on a given task. Toward theoretically grounding these merits, we propose a general setting of recovering linear operators M from noisy vector measurements $y = Mx + w$, where the covariates x may be both non-i.i.d. and non-isotropic. We demonstrate that existing isotropy-agnostic representation learning approaches incur biases on the representation update, which causes the scaling of the noise terms to lose favorable dependence on the number of source tasks. This in turn can cause the sample complexity of representation learning to be bottlenecked by the single-task data size. We introduce an adaptation, **De-bias & Feature-Whiten (DFW)**, of the popular alternating minimization-descent scheme proposed independently in Collins et al. [2021] and Nayer and Vaswani [2022], and establish linear convergence to the optimal representation with noise level scaling down with the *total* source data size. This leads to generalization bounds on the same order as an oracle empirical risk minimizer. We verify the vital importance of DFW on various numerical simulations. In particular, we show that vanilla alternating-minimization descent fails catastrophically even for iid, but mildly non-isotropic data. Our analysis unifies and generalizes prior work, and provides a flexible framework for a wider range of applications, such as in controls and dynamical systems.

1 Introduction

A unifying paradigm belying recent exciting progress in machine learning is learning a common feature space or *representation* for downstream tasks from heterogeneous sources. This forms the core of fields such as meta-learning, transfer learning, and federated learning. A shared theme across these fields is the scarcity of data for a specific task out of many, such that designing individual models for each task is both computationally and statistically inefficient, impractical, or impossible. Under the assumption that these tasks are similar in some way, a natural alternative approach is to use data across many tasks to learn a common component, such that fine-tuning to a given task involves fitting a much smaller model that acts on the common component. Over the last few years, significant attention has been given to framing this problem setting theoretically, providing provable benefits of learning over multiple tasks in the context of linear regression [Collins et al., 2021, Bullins et al., 2019, Du et al., 2020, Tripuraneni et al., 2021, Thekumparampil et al., 2021, Saunshi et al., 2021] and in identification/control of linear dynamical systems [Modi et al., 2021, Chen et al., 2023,

*Corresponding author, email: ttz2@seas.upenn.edu

Zhang et al., 2023]. These works study the problem of *linear representation learning*, where the data for each task is generated noisily from an unknown shared latent subspace, and the goal is to efficiently recover a representation of the latent space $\hat{\Phi}$ from data across different task distributions. For example, in the linear regression setting, one may have data of the form

$$y_i^{(t)} = \theta^{(t)\top} \Phi x_i^{(t)} + \text{noise}, \quad y_i^{(t)} \in \mathbb{R}, x_i^{(t)} \in \mathbb{R}^{d_x}, \Phi \in \mathbb{R}^{r \times d_x},$$

with $i = 1, \dots, N$ iid data points from $t = 1, \dots, T$ task distributions. Since the representation Φ is shared across all tasks, one may expect the generalization error of an approximate representation $\hat{\Phi}$ fit on TN data points to scale as $\frac{d_{\hat{\Phi}}}{TN}$, where $d_{\hat{\Phi}}$ is the number of parameters determining the representation. This is indeed the flavor of statistical guarantees from prior work [Du et al., 2020, Tripuraneni et al., 2021, Thekumparampil et al., 2021, Zhang et al., 2023], which concretely demonstrates the benefit of using data across different tasks.

However, existing work, especially beyond the scalar measurement setting, is limited in one or more important components of their analysis. For example, it is common to assume that the covariates $x_i^{(t)}$ are isotropic across all tasks. Furthermore, statistical analyses often assume access to an empirical risk minimizer, even though the linear representation learning problem is non-convex and ill-posed [Du et al., 2020, Zhang et al., 2023, Maurer et al., 2016]. Our paper addresses these problems under a unified framework of *linear operator recovery*, i.e. recovering linear operators $M \in \mathbb{R}^{d_y \times d_x}$ from (noisy) vector measurements $y = Mx + w$, where the covariates x may not be independent or isotropic. This setting subsumes the scalar measurement setting, and encompasses many fundamental control and dynamical systems problems, such as linear system identification and imitation learning. In particular, the data in these settings are incompatible with the common distributional assumptions (e.g., independence, isotropy) made in prior work.

Contributions: Toward this end, our main contributions are as follows:

- We demonstrate that naive implementation of local methods for linear representation learning fail catastrophically even when the data is iid but mildly non-isotropic. We identify the source of the failure as interaction between terms incurring biases in the representation gradient, which do not scale down with the number of tasks.
- We address these issues by introducing two practical algorithmic adjustments, **De-bias & Feature-Whiten (DFW)**, which provably mitigate the identified issues. We then show that DFW is necessary for gradient-based methods to benefit from the total size of the source dataset.
- We numerically show our theoretical guarantees are predictive of the efficacy of our proposed algorithm, and of the key importance of individual aspects of our algorithmic framework.

Our main result can be summarized by the following descent guarantee for our proposed algorithm.

Theorem 1.1 (main result, informal) *Let $\hat{\Phi}$ be the current estimate of the representation, and Φ_\star the optimal representation. Running one iteration of DFW yields the following improvement*

$$\text{dist}(\hat{\Phi}_+, \Phi_\star) \leq \rho \cdot \text{dist}(\hat{\Phi}, \Phi_\star) + \frac{C}{\sqrt{\# \text{ tasks} \times \# \text{ data per task}}}, \quad \rho \in (0, 1), C > 0.$$

Critically, the second term of the right hand side scales jointly in the number of tasks and datapoints per task, whereas naively implementing other methods may be bottlenecked by a term that scales solely with the amount of data for a single task, which leads to suboptimal sample-efficiency.

1.1 Related Work

Multi-task linear regression: Directly related to our work are results demonstrating the benefits of multi-task learning for linear regression [Collins et al., 2021, Bullins et al., 2019, Du et al., 2020, Tripuraneni et al., 2021, Thekumparampil et al., 2021, Maurer et al., 2016], under the assumption of a shared but unknown linear feature representation. In particular, our proposed algorithm is adapted from the alternating optimization scheme independently in Nayer and Vaswani [2022] and Collins et al. [2021], and extends these results to the vector measurement setting and introduces algorithmic modifications to extend its applicability to non-iid and non-isotropic covariates. We also highlight that in the isotropic linear regression setting, Thekumparampil et al. [2021] provide an alternating minimization scheme that results in near minimax-optimal representation learning. However, the representation update step simultaneously accesses data across tasks, which we avoid in this work due to motivating applications, e.g. distributed learning, that impose locality or data privacy constraints.

Meta/multi-task RL: There is a wealth of literature in reinforcement learning that seeks empirically to solve different tasks with shared parameters [Teh et al., 2017, Hessel et al., 2018, Singh et al., 2020, Deisenroth et al., 2014]. In parallel, there is a body of theoretical work which studies the sample efficiency of representation learning for RL [Lu et al., 2021, Cheng et al., 2022, Maurer et al., 2015]. This line of work considers MDP settings, and thus the specific results are often stated with incompatible assumptions (such as bounded states/cost functions and discrete action spaces), and are suboptimal when instantiated in our setting.

System identification and control: Multi-task learning has gained recent attention in controls, e.g. for adaptive control over similar dynamics [Harrison et al., 2018, Richards et al., 2021, Shi et al., 2021, Muthirayan et al., 2022], imitation learning for linear systems [Zhang et al., 2023, Guo et al., 2023], and notably linear system identification [Modi et al., 2021, Chen et al., 2023, Li et al., 2022, Wang et al., 2022, Xin et al., 2023, Faradonbeh and Modi, 2022]. In many of these works [Li et al., 2022, Wang et al., 2022, Xin et al., 2023], task similarity is quantified by a generic norm closeness of the dynamics matrices, and thus the benefit of multiple tasks extends only to a radius around optimality. Under the existence of a shared representation, our work provides an efficient algorithm and statistical analysis to establish convergence to per-task optimality.

2 Problem Formulation

Notation: the Euclidean norm of a vector x is denoted $\|x\|$. The spectral and Frobenius norms of a matrix A are denoted $\|A\|$ and $\|A\|_F$, respectively. For symmetric matrices A, B , $A \preceq B$ denotes $B - A$ is positive semidefinite. The largest/smallest singular and eigenvalues of a matrix A are denoted $\sigma_{\max}(A)$, $\sigma_{\min}(A)$, and $\lambda_{\max}(A)$, $\lambda_{\min}(A)$, respectively. The condition number of a matrix A is denoted $\kappa(A) := \sigma_{\max}(A)/\sigma_{\min}(A)$. Define the indexing shorthand $[n] := \{1, \dots, n\}$. We use \lesssim, \gtrsim to omit universal numerical factors, and $\tilde{O}(\cdot), \tilde{\Omega}(\cdot)$ to omit polylog factors in the argument. We also use

Regression Model. Let a covariate sequence (also denoted a *trajectory*) be an indexed set $\{x_i\}_{i \geq 1} \subset \mathbb{R}^{d_x}$. We denote a distribution \mathbb{P}_x over covariate sequences, which we assume to have bounded second moments for all $i \geq 1$, i.e. $\mathbb{E}[x_i x_i^\top]$ is finite for all $i \geq 1$. Defining the filtration $\{\mathcal{F}_i\}_{i \geq 0}$ where $\mathcal{F}_i := \sigma(\{x_k\}_{k=1}^{i+1}, \{w_k\}_{k=1}^i)$ is the σ -algebra generated by the covariates up to $i + 1$

and noise up to i , we assume that $\{w_i\}_{i \geq 1}$ is a σ_w^2 -subgaussian martingale difference sequence (MDS):

$$\mathbb{E} \left[v^\top w_i \mid \mathcal{F}_{i-1} \right] = 0, \quad \mathbb{E} \left[\exp \left(\lambda v^\top w_i \right) \mid \mathcal{F}_{i-1} \right] \leq \exp \left(\lambda^2 \|v\|^2 \sigma_w^2 \right) \text{ a.s. } \forall \lambda \in \mathbb{R}, v \in \mathbb{R}^{d_y}.$$

Assuming a ground truth operator $M_\star \in \mathbb{R}^{d_y \times d_x}$, our observation model is given by

$$y_i = M_\star x_i + w_i, \quad i \geq 1,$$

for y_i the *labels*, and w_i the *label noise*. We further define $\Sigma_{x,N} := \frac{1}{N} \sum_{i=1}^N \mathbb{E}[x_i x_i^\top]$. When the marginal distributions of x_i , $i \geq 1$ are identical, we denote $\Sigma_x \equiv \Sigma_{x,N}$.

Multi-Task Operator Recovery. We consider the following instantiation of the above linear operator regression model over multiple tasks. In particular, we consider heterogeneous data $\{(x_i^{(t)}, y_i^{(t)})\}_{i=1, t=1}^{N,T}$, consisting of trajectories of length N , generated independently across $t = 1, \dots, T$ task distributions. For notational convenience, we assume that the length of trajectories N is the same across training tasks. For each task t , the observation model is

$$y_i^{(t)} = M_\star^{(t)} x_i^{(t)} + w_i^{(t)}, \quad (1)$$

where $M_\star^{(t)} = F_\star^{(t)} \Phi_\star$ admits a decomposition into a ground-truth representation $\Phi_\star \in \mathbb{R}^{r \times d_x}$ common across all tasks $t \in [T]$ and a task-specific weight matrix $F_\star^{(t)} \in \mathbb{R}^{d_y \times r}$, $r \leq d_x$. We denote the joint distribution over covariates and observations $\{x_i^{(t)}, y_i^{(t)}\}_{i \geq 1}$ by $\mathbb{P}_{x,y}^{(t)}$. We assume that the representation Φ_\star is normalized to have orthonormal rows to prevent boundedness issues, since $F_\star^{(t)'} = F_\star^{(t)} Q^{-1}$, $\Phi_\star' = Q \Phi_\star$ are also valid decompositions for any invertible $Q \in \mathbb{R}^{r \times r}$. To measure closeness of an approximate representation $\hat{\Phi}$ to optimality, we define a subspace metric.

Definition 2.1 (Subspace Distance [Collins et al., 2021, Stewart and Sun, 1990]) *Let $\Phi, \Phi_\star \in \mathbb{R}^{r \times d_x}$ be matrices whose rows are orthonormal. Furthermore, let $\Phi_{\star,\perp} \in \mathbb{R}^{(d_x-r) \times d_x}$ be a matrix such that $[\Phi_\star^\top \quad \Phi_{\star,\perp}^\top]$ is an orthogonal matrix. Define the distance between the subspaces spanned by the rows of Φ and Φ_\star by*

$$\text{dist}(\Phi, \Phi_\star) := \|\Phi \Phi_{\star,\perp}^\top\|_2 \quad (2)$$

In particular, the subspace distance quantitatively captures the alignment between two subspaces, interpolating smoothly between 0 (occurring iff $\text{span}(\Phi_\star) = \text{span}(\hat{\Phi})$) and 1 (occurring iff $\text{span}(\Phi_\star) \perp \text{span}(\hat{\Phi})$). We define the task-specific stacked vector notation by capital letters, e.g.,

$$X^{(t)} = \begin{bmatrix} x_1^{(t)} & \dots & x_i^{(t)} & \dots & x_N^{(t)} \end{bmatrix}^\top \in \mathbb{R}^{N \times d_x}.$$

The goal of multi-task operator recovery is to estimate $\{F_\star^{(t)}\}_{t=1}^T$ and Φ_\star from data collected across multiple tasks $\{(x_i^{(t)}, y_i^{(t)})\}_{i=1}^N$, $t = 1, \dots, T$. Some prior works [Du et al., 2020, Zhang et al., 2023, Maurer et al., 2016] assume access to an empirical risk minimization oracle, i.e. access to

$$\{\hat{F}^{(t)}\}_{t=1}^T, \hat{\Phi} \in \underset{\{F^{(t)}\}, \Phi}{\text{argmin}} \sum_{t=1}^T \sum_{i=1}^N \left\| y_i^{(t)} - F^{(t)} \Phi x_i^{(t)} \right\|^2,$$

focusing on the statistical generalization properties of an ERM solution. However, the above optimization is non-convex even in the linear setting, and thus it is imperative to design and analyze

efficient algorithms for recovering optimal matrices $\{F_\star^{(t)}\}_{t=1}^T$ and Φ_\star . To address this problem in the linear regression setting, various works, e.g. **FedRep** [Collins et al., 2021], **AltGD-Min** [Nayer and Vaswani, 2022], propose an alternating minimization-descent scheme, where on a fresh data batch, the weights $\{\hat{F}^{(t)}\}$ are computed on task-specific (“local”) data via least-squares, and an estimate of the representation gradient is subsequently computed with respect to task-specific data and averaged across tasks to perform gradient descent on the representation parameters. This algorithmic framework is intuitive, and thus forms a reasonable starting point toward a provably sample-efficient algorithm in our setting.

3 Sample-Efficient Linear Representation Learning

We begin by describing the vanilla alternating minimization-descent scheme proposed in Collins et al. [2021]. We show that in our setting with label noise and non-isotropy, interaction terms arise in the representation gradient, which cause biases to form that do not scale down with the number of tasks T . In §3.2, we propose alterations to the scheme to remove these biases, which we then show in §3.3 lead to fast convergence rates that allow us to recover near-oracle ERM generalization bounds.

3.1 Perils of (Vanilla) Gradient Descent on the Representation

We begin with a summary of the main components of an alternating minimization-descent method analogous to **FedRep** [Collins et al., 2021] and **AltGD-Min** [Nayer and Vaswani, 2022]. During each optimization round, a new data batch is sampled for each task: $\{(x_i^{(t)}, y_i^{(t)})\}_{i=1}^N$, $t \in [T]$. We then compute task-specific weights $\hat{F}^{(t)}$ on the corresponding dataset, keeping the current representation estimate $\hat{\Phi}$ fixed. For example, $\hat{F}^{(t)}$ may be the least-squares weights conditioned on $\hat{\Phi}$ [Collins et al., 2021]. Define $z_i^{(t)} := \hat{\Phi} x_i^{(t)}$, and the empirical covariance matrices $\hat{\Sigma}_x^{(t)} := \frac{1}{N} X^{(t)\top} X^{(t)}$, $\hat{\Sigma}_z^{(t)} := \frac{1}{N} Z^{(t)\top} Z^{(t)}$. The least squares solution $\hat{F}^{(t)}$ is given by the convex quadratic minimization

$$\begin{aligned} \hat{F}^{(t)} &= \operatorname{argmin}_F \sum_{i=1}^N \left\| y_i^{(t)} - F z_i^{(t)} \right\|^2 \\ &= F_\star^{(t)} \Phi_\star X^{(t)\top} Z^{(t)} (\hat{\Sigma}_z^{(t)})^{-1} + W^{(t)\top} Z^{(t)} (\hat{\Sigma}_z^{(t)})^{-1}, \end{aligned} \quad (3)$$

where we derive (3) through standard matrix calculus [Petersen et al., 2008] and expanding (1). For each task, we then fix the weight matrix $\hat{F}^{(t)}$ and perform a descent step with respect to the representation conditioned on the local data. The resulting representations are averaged across tasks to form the new representation. When the descent direction is the gradient, the update rule is given by

$$\bar{\Phi}_+^{(t)} = \hat{\Phi} - \frac{\eta}{2N} \nabla_{\Phi} \left\| \sum_{i=1}^N y_i^{(t)} - \hat{F}^{(t)} \hat{\Phi} x_i^{(t)} \right\|^2, \quad \bar{\Phi}_+ = \frac{1}{T} \sum_{t=1}^T \bar{\Phi}_+^{(t)} \quad (4)$$

where $\eta > 0$ is a given step size. We normalize $\bar{\Phi}_+$ to have orthonormal rows, e.g. by (thin/reduced) QR decomposition [Trefethen and Bau, 2022], to produce the final output $\hat{\Phi}_+$, i.e. $\bar{\Phi}_+ = R \hat{\Phi}_+$, $R \in \mathbb{R}^{r \times r}$, leading to

$$R \hat{\Phi}_+ = \hat{\Phi} - \frac{\eta}{T} \sum_{t=1}^T \hat{F}^{(t)\top} \left(\hat{F}^{(t)} \hat{\Phi} - F_\star^{(t)} \Phi_\star \right) \hat{\Sigma}_x^{(t)} - \frac{\eta}{NT} \sum_{t=1}^T \hat{F}^{(t)\top} W^{(t)\top} X^{(t)}. \quad (5)$$

As in Collins et al. [2021], we right-multiply both sides of (5) by $\Phi_{*,\perp}^\top$, recalling $\|\Phi\Phi_{*,\perp}^\top\|_2 =: \text{dist}(\Phi, \Phi_*)$. Crucially, Collins et al. [2021] assume $x_i^{(t)}$ has mean 0 and identity covariance, and $w_i^{(t)} \equiv 0$ across i, t . Therefore, the label noise terms $\hat{F}^{(t)\top}W^{(t)\top}X^{(t)}$ disappear, and the sample covariance for each task $\hat{\Sigma}_x^{(t)}$ concentrates to identity. Under these assumptions, we get

$$\begin{aligned} \|R\hat{\Phi}_+ \Phi_{*,\perp}^\top\| &= \left\| \hat{\Phi}\Phi_{*,\perp}^\top - \frac{\eta}{T} \sum_{t=1}^T \hat{F}^{(t)\top} \left(\hat{F}^{(t)}\hat{\Phi} - F_*^{(t)}\Phi_* \right) \hat{\Sigma}_x^{(t)}\Phi_{*,\perp}^\top \right\| \\ &\lesssim \underbrace{\left\| I - \frac{\eta}{T} \sum_{t=1}^T \hat{F}^{(t)\top}\hat{F}^{(t)} \right\|}_{\text{Contraction term}} \underbrace{\text{dist}(\hat{\Phi}, \Phi_*) + \mathcal{O}\left(\frac{1}{T} \sum_{t=1}^T \|\hat{\Sigma}_x^{(t)} - I_{d_x}\|\right)}_{\text{Covariance concentration term}}. \end{aligned}$$

where we note $\Phi_*\Phi_{*,\perp}^\top = 0$. Under appropriate choice of η and bounding the effect of the orthonormalization factor R , linear convergence to the optimal representation can be established. However, two issues arise when label noise $w_i^{(t)}$ is introduced and when $x_i^{(t)}$ has non-identity covariance.

1. When *label noise* $w_i^{(t)}$ is present, since $\hat{F}^{(t)}$ is computed on $Y^{(t)}, X^{(t)}$, the gradient noise term is generally biased: $\frac{1}{NT}\mathbb{E}[\hat{F}^{(t)}W^{(t)\top}X^{(t)}] \neq 0$. Even in the simple case that all task distributions $\mathbb{P}_{x,y}^{(t)}$ are identical, $\frac{\eta}{NT}\sum_{t=1}^T \hat{F}^{(t)\top}W^{(t)\top}X^{(t)}$ concentrates to its bias, and thus for large T the size of noise term is bottlenecked at $\frac{\eta}{NT}\mathbb{E}\left[\left\|\hat{F}^{(t)\top}W^{(t)\top}X^{(t)}\right\|\right]$. This critically causes the noise term to lose scaling in the *number of tasks* T , even when the tasks are identical.
2. When $x_i^{(t)}$ has *non-identity covariance*, the decomposition into a contraction and covariance concentration term no longer holds, since generally $\Phi_*\mathbb{E}[\hat{\Sigma}_x^{(t)}]\Phi_{*,\perp}^\top \neq 0$. This causes a term whose norm otherwise concentrates around 0 in the isotropic case to scale with $\lambda_{\max}(\hat{\Sigma}_x^{(t)}) - \lambda_{\min}(\hat{\Sigma}_x^{(t)})$ in the worst case. Unlike prior work that assumes identical distribution of covariates $x_i^{(t)}$ across tasks, this issue cannot be circumvented by whitening the covariates $x_i^{(t)}$, as shifting the task-specific covariance factor to the operator $F_*^{(t)}\Phi_*\Sigma_x^{(t)1/2}$ in general ruins the shared representation spanned by Φ_* .

This motivates modifying the representation update beyond following the vanilla stochastic gradient.

3.2 A Task-Efficient Algorithm: De-bias & Feature-whiten

In the previous section, we identified two fundamental issues: 1. the bias introduced by computing the least squares weights and representation update on the same data batch, and 2. the nuisance term introduced by non-identity second moments of the covariates $x_i^{(t)}$. Toward addressing the first issue, we introduce a “de-biasing” step, where each agent computes the least squares weights $\hat{F}^{(t)}$ and the representation update on *independent* batches of data, e.g. disjoint subsets of trajectories. To address the second issue, we introduce a “feature-whitening” adaptation [LeCun et al., 2002], where the gradient estimate sent by each agent is pre-conditioned by its inverse sample covariance matrix. Combining these two adaptations, the representation update becomes

$$R\hat{\Phi}_+ = \hat{\Phi} - \frac{\eta}{T} \sum_{t=1}^T \hat{F}^{(t)\top} \left(\hat{F}^{(t)}\hat{\Phi} - F_*^{(t)}\Phi_* \right) - \frac{\eta}{T} \sum_{t=1}^T \hat{F}^{(t)\top}W^{(t)\top}X^{(t)} \left(\hat{\Sigma}_x^{(t)} \right)^{-1}, \quad (6)$$

where we assume $\{\hat{F}^{(t)}\}$ are computed on independent data using the aforementioned batching strategy. We comment that this “pre-conditioning by the inverse sample covariance” step bears

striking resemblance to various algorithms applied to dynamical systems, e.g. Quasi-Newton method for Generalized Linear Models [Kowshik et al., 2021], natural policy gradient for linear-quadratic systems [Fazel et al., 2018]. Curiously, the various motivations of this step differ entirely between all of these works; for example, the purpose of this step in our work arises even for independent data. When $x_i^{(t)}, w_i^{(t)}, t = 1, \dots, T$, are all mutually independent, then the first two terms of the update form the contraction, and the last term is an average of *zero-mean* least-squares-error-like terms over tasks, which can be studied using standard tools [Abbasi-Yadkori et al., 2011, Abbasi-Yadkori, 2013]. This culminates in convergence rates that scale favorably with the number of tasks (§3.3). To operationalize our proposed adaptations, let $D^{(t)} = \{(x_i^{(t)}, y_i^{(t)})\}_{i=1}^N, t \in [T]$, be a dataset available to each agent. For the weights de-biasing step, we sub-sample trajectories $\mathcal{N}_1 \subset [N], |\mathcal{N}_1| := N_1$. For each agent, we compute least-squares weights from \mathcal{N}_1 . We then sub-sample trajectories $\mathcal{N}_2 \subset [N] \setminus \mathcal{N}_1, |\mathcal{N}_2| = N_2$, and compute the task-conditioned representation gradients from \mathcal{N}_2 .

$$\hat{F}^{(t)} = \operatorname{argmin}_F \sum_{i \in \mathcal{N}_1} \|y_i^{(t)} - F z_i^{(t)}\|^2, \quad \hat{\mathcal{G}}_{\mathcal{N}_2}^{(t)} = \nabla_{\Phi} \frac{1}{2} \left\| \sum_{i \in \mathcal{N}_2} y_i^{(t)} - \hat{F}^{(t)} \hat{\Phi} x_i^{(t)} \right\|^2. \quad (7)$$

Lastly, each agent updates its local representation via a feature-whitened gradient step to yield $\bar{\Phi}_+^{(t)}$. The global representation update is computed by averaging the updated task-conditioned representations $\bar{\Phi}_+^{(t)}$ and performing orthonormalization:

$$\begin{aligned} \bar{\Phi}_+^{(t)} &:= \hat{\Phi} - \eta \hat{\mathcal{G}}_{\mathcal{N}_2}^{(t)} \left(\hat{\Sigma}_{x, \mathcal{N}_2}^{(t)} \right)^{-1}, \quad R \hat{\Phi}_+ = \frac{1}{T} \sum_{t=1}^T \bar{\Phi}_+^{(t)} \text{ s.t. } \hat{\Phi}_+^\top \hat{\Phi}_+ = I_r \\ &\iff \hat{\Phi}_+, R = \text{thin_QR} \left(\frac{1}{T} \sum_{t=1}^T \bar{\Phi}_+^{(t)} \right), \end{aligned} \quad (8)$$

We summarize the full algorithm in Algorithm 1. The above de-biasing and feature whitening steps ensure that the expectation of the representation update (6) is a contraction (with high probability):

$$\begin{aligned} R \hat{\Phi}_+ \Phi_{\star, \perp}^\top &= \left(I - \frac{\eta}{T} \sum_{t=1}^T \hat{F}^{(t)\top} \hat{F}^{(t)} \right) \hat{\Phi} \Phi_{\star, \perp}^\top - \frac{\eta}{T} \sum_{t=1}^T \hat{F}^{(t)\top} W^{(t)\top} X^{(t)} \left(\hat{\Sigma}_x^{(t)} \right)^{-1} \Phi_{\star, \perp}^\top \\ \implies \mathbb{E} \left[\text{dist}(\hat{\Phi}_+, \Phi_\star) \right] &= \mathbb{E} \left[\left\| R^{-1} \left(I - \frac{\eta}{T} \sum_{t=1}^T \hat{F}^{(t)\top} \hat{F}^{(t)} \right) \right\| \right] \text{dist}(\hat{\Phi}, \Phi_\star), \end{aligned} \quad (9)$$

where the task and trajectory-wise independence ensures that the variance of the gradient scales inversely in NT .

Remark 3.1 (Choice of weights $\hat{F}^{(t)}$ vs. descent rate) *By observing the contraction expression (9), the contraction rate is seemingly solely controlled by the (average) conditioning of the weight matrices $\hat{F}^{(t)}$. Since the choice of algorithm for computing $\hat{F}^{(t)}$ is user-determined, this motivates choosing well-conditioned $\hat{F}^{(t)}$. However, the hidden trade-off lies in the orthonormalization factor R ; arbitrary $\hat{F}^{(t)}$ may lead to R that undoes progress. As in Collins et al. [2021], we analyze $\hat{F}^{(t)}$ generated by representation-conditioned least squares (7), but an optimal balance between conditioning of $\hat{F}^{(t)}$ and R can be struck by ℓ^2 -regularized least squares weights $\hat{F}^{(t)}(\lambda)$ (see, e.g. Hsu et al. [2012]).*

Algorithm 1 De-biased & Feature-whitened (DFW) Alt. Minimization-Descent

- 1: **Input:** step sizes $\{\eta_k\}_{k \geq 1}$, batch sizes $\{N_k\}_{k \geq 1}$, initial estimate $\hat{\Phi}_0$.
 - 2: **for** $k = 1, \dots, K$ **do**
 - 3: **for** $t \in [T]$ **(in parallel)** **do**
 - 4: Obtain samples $\{(x_i^{(t)}, y_i^{(t)})\}_{i=1}^{N_k}$.
 - 5: Partition trajectories $[N_k] = \mathcal{N}_{k,1} \sqcup \mathcal{N}_{k,2}$.
 - 6: Compute $\hat{F}_k^{(t)}$, e.g. via least squares on $\mathcal{N}_{k,1}$ (7).
 - 7: Compute task-conditioned representation gradient $\hat{\mathcal{G}}_{\mathcal{N}_{k,2}}^{(t)}$ on $\mathcal{N}_{k,2}$ (7).
 - 8: Compute task-conditioned representation update $\bar{\Phi}_k^{(t)}$ (8).
 - 9: **end for**
 - 10: $\hat{\Phi}_{k,-} \leftarrow \text{thin_QR} \left(\frac{1}{T} \sum_{t=1}^T \bar{\Phi}_k^{(t)} \right)$.
 - 11: **end for**
 - 12: **return** Representation estimate $\hat{\Phi}_K$.
-

3.3 Algorithm Guarantees

We present our main result in the form of convergence guarantees for Algorithm 1. We begin by defining a standard measure of dependency along covariate sequences via β -mixing.

Definition 3.1 (β -mixing) Let $\{x_i\}_{i \geq 1}$ be a \mathbb{R}^d -valued discrete-time stochastic process adapted to filtration $\{\mathcal{F}_i\}_{i=1}^\infty$. We denote the stationary distribution ν_∞ . We define the β -mixing coefficient

$$\beta(k) := \sup_{i \geq 1} \mathbb{E}_{\{x_\ell\}_{\ell=1}^i} \left[\left\| \mathbb{P}_{x_{i+k}}(\cdot \mid \mathcal{F}_i) - \nu_\infty \right\|_{\text{tv}} \right], \quad (10)$$

where $\|\cdot\|_{\text{tv}}$ denotes the total variation distance between probability measures.

Intuitively, the β -mixing coefficient measures how quickly on average a process converges to its stationary distribution along any sample path. To instantiate our bounds, we make the following assumptions on the covariates.

Assumption 3.1 (Subgaussian covariates, geometric mixing) Given number of tasks T and per-task samples N , we assume the marginal distributions of $x_i^{(t)}$ to be identical with zero-mean, covariance $\Sigma_x^{(t)}$, and to γ^2 -subgaussian across all $i \in [N], t \in [T]$:

$$\mathbb{E}[x_i^{(t)}] = 0, \quad \mathbb{E} \left[\exp \left(\lambda v^\top x_i^{(t)} \right) \right] \leq \exp \left(\lambda^2 \|v\|^2 \gamma^2 \right) \quad \text{a.s. } \forall \lambda \in \mathbb{R}, v \in \mathbb{R}^{d_x}.$$

Furthermore, we assume the process $\{x_i^{(t)}\}_{i \geq 1}$ is geometrically β -mixing with $\beta^{(t)}(k) \leq \Gamma^{(t)} \mu^{(t)k}$, $\Gamma^{(t)} > 0$, $\mu^{(t)} \in [0, 1)$, for each task $t \in [T]$. Lastly, we define $\tau_{\text{mix}}^{(t)} := \left(\frac{\log(\Gamma^{(t)} N / \delta)}{\log(1/\mu^{(t)})} \vee 1 \right)$.

Notably, these assumptions subsume fundamental problems in learning over (stable) dynamical systems, in particular linear system identification and imitation learning, where non-iid and non-isotropy across tasks are unavoidable. We discuss these instantiations in depth in Appendix B. As in prior work, our final convergence rates depend on a notion of task diversity.

Definition 3.2 (Task diversity) We define the quantities

$$\lambda_{\min}^{\mathbf{F}} := \lambda_{\min} \left(\frac{1}{T} \sum_{t=1}^T F_\star^{(t)\top} F_\star^{(t)} \right), \quad \lambda_{\max}^{\mathbf{F}} := \lambda_{\max} \left(\frac{1}{T} \sum_{t=1}^T F_\star^{(t)\top} F_\star^{(t)} \right). \quad (11)$$

As hinted by Equation (9), our proof strategy boils down to bounding the various terms in the update rule of DFW; in particular, the “contraction factor” $I - \frac{\eta}{T} \sum_{t=1}^T \hat{F}^{(t)\top} \hat{F}^{(t)}$, the task-averaged noise term $\frac{1}{T} \sum_{t=1}^T \hat{F}^{(t)\top} W^{(t)\top} X^{(t)} (\hat{\Sigma}_x^{(t)})^{-1}$, and lastly the effect of orthonormalization R . Starting with the contraction factor, we observe expanding the least-squares weights yields:

$$\begin{aligned} \hat{F}^{(t)} &= F_\star^{(t)} \Phi_\star X^{(t)\top} Z^{(t)} (\hat{\Sigma}_z^{(t)})^{-1} + W^{(t)\top} Z^{(t)} (\hat{\Sigma}_z^{(t)})^{-1} \\ &= F_\star^{(t)} \Phi_\star \hat{\Phi}^\top + F_\star^{(t)} \Phi_\star \hat{\Phi}_\perp^\top \hat{\Phi}_\perp X^{(t)\top} Z^{(t)} (\hat{\Sigma}_z^{(t)})^{-1} + W^{(t)\top} Z^{(t)} (\hat{\Sigma}_z^{(t)})^{-1}. \end{aligned}$$

Intuitively speaking, the least-squares weights decomposes into a term proportional to $F_\star^{(t)}$, an error term arising from misspecification scaling with $\|\Phi_\star \hat{\Phi}_\perp^\top\| = \text{dist}(\hat{\Phi}, \Phi_\star)$, and a zero-mean least-squares error term scaling with $\sigma_w^{(t)}$. Therefore, inverting bounds on the error terms into burn-in conditions, we get after some computation the following bound.

Lemma 3.1 (Contraction factor bound) *Let Assumption 3.1 hold. If the following burn-in conditions hold*

$$\begin{aligned} \text{dist}(\hat{\Phi}, \Phi_\star) &\leq \frac{1}{100} \sqrt{\frac{\lambda_{\min}^{\mathbf{F}}}{\lambda_{\max}^{\mathbf{F}}}} \max_t \kappa(\Sigma_x^{(t)})^{-1} \\ N_1 &\gtrsim \max_t \tau_{\text{mix}}^{(t)} \cdot \max \left\{ \gamma^4 (r + \log(T/\delta)), \lambda_{\min}^{\mathbf{F}}^{-1} \frac{1}{T} \sum_{t=1}^T \frac{\sigma_w^{(t)2} (d_y + r + \log(T/\delta))}{\lambda_{\min}(\Sigma_x^{(t)})} \right\}, \end{aligned}$$

then, for step-size satisfying $\eta \leq 0.956 \lambda_{\max}^{\mathbf{F}}^{-1}$, with probability at least $1 - \delta$, we have

$$\left\| I_{d_x} - \eta \frac{1}{T} \sum_{t=1}^T \hat{F}^{(t)\top} \hat{F}^{(t)} \right\| \leq (1 - 0.954 \eta \lambda_{\min}^{\mathbf{F}}).$$

Setting $\eta \approx \lambda_{\max}^{\mathbf{F}}^{-1}$, we observe that the bound on the contraction factor is approximately $1 - c \frac{\lambda_{\min}^{\mathbf{F}}}{\lambda_{\max}^{\mathbf{F}}}$, which is the best one can hope for in the spectral norm. Furthermore, we note that past the burn-in, the contraction rate is independent of the data-size $N_1 = |\mathcal{N}_1|$ used to compute the weights, implying that contraction holds as long as the least-squares weights are “good enough” (tying back to Remark 3.1), further implying N_1 can be held fixed across rounds of DFW.

To bound the DFW noise term, we observe that for each task, $\hat{F}^{(t)\top} W^{(t)\top} X^{(t)} (\hat{\Sigma}_x^{(t)})^{-1}$ is an $r \times d_x$ matrix-valued self-normalized martingale [Abbasi-Yadkori, 2013]. Importantly, by the de-biasing step, the weights $\hat{F}^{(t)}$ are mutually independent of the processes $W^{(t)}, X^{(t)}$ in the independent covariates setting. Similarly to the contraction factor, assuming a burn-in on $\text{dist}(\hat{\Phi}, \Phi_\star)$ and N_1 , the subgaussian constant of $\hat{F}^{(t)\top} w_i^{(t)}$ can be bounded by, say, $2 \|F_\star^{(t)}\|_2 \sigma_w^{(t)2}$. By realizability (1), we see that in the independent covariates setting, $\hat{F}^{(t)\top} W^{(t)\top} X^{(t)} (\hat{\Sigma}_x^{(t)})^{-1}$ is a *zero-mean* process that is bounded with high-probability. Therefore, applying a matrix Hoeffding inequality [Tropp, 2011] across tasks T crucially yields a bound on the noise term that benefits from more tasks T .

Proposition 3.1 (Noise term bound) *Let Assumption 3.1 hold. Assume*

$$\begin{aligned} \text{dist}(\hat{\Phi}, \Phi_\star) &\leq \max_t \frac{1}{100} \kappa(\Sigma_x^{(t)})^{-1} \\ N_1 &\gtrsim \max_t \tau_{\text{mix}}^{(t)} \cdot \max \left\{ \gamma^4 (r + \log(T/\delta)), \max_t \frac{\sigma_w^{(t)2}}{\|F_\star^{(t)}\|_2^2 \lambda_{\min}(\Sigma_x^{(t)})} (d_y + r + \log(T/\delta)) \right\}, \\ N_2 &\gtrsim \max_t \tau_{\text{mix}}^{(t)} \cdot \gamma^4 (d_x + \log(T/\delta)). \end{aligned}$$

Then, with probability at least $1 - \delta$,

$$\left\| \frac{1}{T} \sum_{t=1}^T \hat{F}^{(t)\top} W_{\mathcal{N}_2}^{(t)\top} X_{\mathcal{N}_2}^{(t)} \left(\hat{\Sigma}_{x, \mathcal{N}_2}^{(t)} \right)^{-1} \right\| \lesssim \sigma_{\text{avg}} \sqrt{\frac{d_x + \log(T/\delta)}{TN_2} \log\left(\frac{d_x}{\delta}\right)},$$

where $\sigma_{\text{avg}} := \sqrt{\frac{1}{T} \sum_{t=1}^T \frac{\tau_{\text{mix}}^{(t)} \sigma_w^{(t)2} \|F_\star^{(t)}\|^2}{\lambda_{\min}(\Sigma_x^{(t)})}}$ is the task-averaged noise-level.

The final piece of the proof lies in bounding the orthonormalization factor R . A key observation is that $RR^\top = (R\hat{\Phi}_+)(R\hat{\Phi}_+)^{\top}$, where $R\hat{\Phi}_+$ is precisely the output of the preconditioned gradient step on $\hat{\Phi}$ (6). Roughly speaking, we observe that the RHS of (6) is composed of three terms, the first of which $\hat{\Phi}$ satisfies $\hat{\Phi}\hat{\Phi}^\top = I_r$, the second which scales with $\frac{1}{T} \sum_{t=1}^T \hat{F}^{(t)}\hat{\Phi} - F_\star^{(t)}\Phi_\star$, and the third that is the task-averaged self-normalized martingale term. Therefore, by re-invoking tools used in Lemma 3.1 and Proposition 3.1, we find that under similar burn-in conditions, the orthogonalization factor is a small perturbation to identity, thus leaving the contraction rate and noise term essentially unaffected.

Lemma 3.2 *Let Assumption 3.1 hold. Let the following burn-in conditions hold:*

$$\begin{aligned} \text{dist}(\hat{\Phi}, \Phi_\star) &\leq \frac{1}{100} \sqrt{\frac{\lambda_{\min}^{\mathbf{F}}}{\lambda_{\max}^{\mathbf{F}}} \max_t \kappa(\Sigma_x^{(t)})^{-1}} \\ N_1 &\gtrsim \max_t \tau_{\text{mix}}^{(t)} \cdot \max\left\{\gamma^4 (r + \log(T/\delta)), \bar{\sigma}_{\mathbf{F}}^2 (d_y + r + \log(T/\delta))\right\}, \\ N_2 &\gtrsim \max_t \tau_{\text{mix}}^{(t)} \cdot \max\left\{\gamma^4 (d_x + \log(T/\delta)), \lambda_{\min}^{\mathbf{F}}^{-1} \frac{\sigma_{\text{avg}}^2}{T} (d_x + \log(T/\delta)) \log\left(\frac{d_x}{\delta}\right)\right\}, \end{aligned}$$

where $\bar{\sigma}_{\mathbf{F}}^2 := \max\left\{\max_t \frac{\sigma_w^{(t)2}}{\|F_\star^{(t)}\|^2 \lambda_{\min}(\Sigma_x^{(t)})}, \frac{1}{T} \sum_{t=1}^T \frac{\sigma_w^{(t)2}}{\lambda_{\min}^{\mathbf{F}} \lambda_{\min}(\Sigma_x^{(t)})}\right\}$. Then, given $\eta \leq 0.956 \lambda_{\max}^{\mathbf{F}}^{-1}$, with probability at least $1 - \delta$, we have the following bound on the orthogonalization factor R :

$$\|R^{-1}\| \leq (1 - 0.0575\eta \lambda_{\min}^{\mathbf{F}})^{-1/2}.$$

Putting all the pieces together, we now present our main result regarding the subspace distance improvement from running one iteration of DFW.

Theorem 3.1 (Main result) *Let Assumption 3.1 hold, and $\sigma_{\text{avg}}^2, \bar{\sigma}_{\mathbf{F}}^2$ be as defined in Proposition 3.1 and Lemma 3.2. Let the following burn-in conditions hold:*

$$\begin{aligned} \text{dist}(\hat{\Phi}, \Phi_\star) &\leq \frac{1}{100} \sqrt{\frac{\lambda_{\min}^{\mathbf{F}}}{\lambda_{\max}^{\mathbf{F}}} \max_t \kappa(\Sigma_x^{(t)})^{-1}} \\ N_1 &\gtrsim \max_t \tau_{\text{mix}}^{(t)} \cdot \max\left\{\gamma^4 (r + \log(T/\delta)), \bar{\sigma}_{\mathbf{F}}^2 (d_y + r + \log(T/\delta))\right\}, \\ N_2 &\gtrsim \max_t \tau_{\text{mix}}^{(t)} \cdot \max\left\{\gamma^4 (d_x + \log(T/\delta)), \lambda_{\min}^{\mathbf{F}}^{-1} \frac{\sigma_{\text{avg}}^2}{T} (d_x + \log(T/\delta)) \log\left(\frac{d_x}{\delta}\right)\right\}, \end{aligned}$$

Then, given step-size satisfying $\eta \leq 0.956 \lambda_{\max}^{\mathbf{F}}^{-1}$, running an iteration of DFW yields an updated representation $\hat{\Phi}_+$ that satisfies with probability at least $1 - \delta$:

$$\text{dist}(\hat{\Phi}_+, \Phi_\star) \leq (1 - 0.897\eta \lambda_{\min}^{\mathbf{F}}) \text{dist}(\hat{\Phi}, \Phi_\star) + C \cdot \sigma_{\text{avg}} \sqrt{\frac{d_x + \log(T/\delta)}{TN_2} \log\left(\frac{d_x}{\delta}\right)},$$

where $C > 0$ is a universal constant.

The full proofs of Theorem 3.1 and the component results are mapped out in Appendix A. Some comments are in order. We specifically highlight the benefit of multi-task data in blue. Furthermore, the dependence on N_1 appears only in the burn-in, implying the amount of data used to compute the weights $\hat{F}^{(t)}$ need not grow, and only N_2 —the amount of data used to perform the preconditioned gradient step—needs to grow to monotonically decrease the subspace distance. This is perhaps surprising, as this implies that reconstructing the operator from the intermediate weights and representations $\hat{M}^{(t)} = \hat{F}^{(t)}\hat{\Phi}$ need not converge to $M_\star^{(t)}$ for DFW to converge to the optimal representation (cf. Appendix A.4.1).

Remark 3.2 (Initialization) *We note that Theorem 3.1 relies on the representation $\hat{\Phi}$ being sufficiently close to Φ_\star . We do not address this issue in this paper, and refer to Collins et al. [2021], Tripuraneni et al. [2021], Thekumparampil et al. [2021] for initialization schemes in the iid linear regression setting. Our experiments suggest that initialization is often unnecessary, which mirrors the experimental findings in Thekumparampil et al. [2021, Sec. 6]. We leave constructing an initialization scheme for our general setting, or showing whether it is unnecessary, to future work.*

Remark 3.3 (Burn-in dependence on d_x) *We remark that the burn-in requirement on N_2 scales linearly with the covariate dimension d_x . This is larger than the $\Omega(r)$ requirements in the algorithm/analysis in Collins et al. [2021], Thekumparampil et al. [2021], which we emphasize critically impose isotropy across all covariates. In the case of DFW, the d_x dependence arises for a fundamental reason: when $N_2 < d_x$, then postmultiplying each task’s representation gradient by $(\hat{\Sigma}_x^{(t)})^\dagger$ yields subspace distance error terms scaling as $\hat{\Phi}\mathcal{P}_{\text{range}(\hat{\Sigma}_x^{(t)})}\Phi_{\star,\perp}^\top$ instead of $\hat{\Phi}\Phi_{\star,\perp}^\top$. Crucially, $\hat{\Phi}\mathcal{P}_{\text{range}(\hat{\Sigma}_x^{(t)})}\Phi_{\star,\perp}^\top$ is an unbiased estimator of $\hat{\Phi}\Phi_{\star,\perp}^\top$ only if $x_i^{(t)}$ is isotropic, and thus improvement in the subspace distance can only be guaranteed for non-isotropic $x_i^{(t)}$ when $N_2 \geq d_x$. We leave as an open question whether an efficient algorithm for linear representation learning can be posed/analyzed for non-isotropic covariates in the low per-task data regime $N < d_x$.*

A key benefit of having the variance term in Theorem 3.1 scale properly in N, T is that we may construct representations on fixed datasets whose error scales on the same order as the oracle empirical risk minimizer by running Algorithm 1 on appropriately partitioned subsets of a given dataset.

Corollary 3.1 (Approximate ERM) *Let the assumptions of Theorem 3.1 hold. Let $\hat{\Phi}_0$ be an initial representation satisfying $\text{dist}(\hat{\Phi}_0, \Phi_\star) < \nu$, and define $\rho := 1 - 0.857 \frac{\lambda_{\text{F}}^{\text{min}}}{\lambda_{\text{F}}^{\text{max}}}$. Let $\mathbf{D} := \{\{(x_i^{(t)}, y_i^{(t)})\}_{i=1}^N\}_{t \in [T]}$ be a given dataset. There exists a partition of \mathbf{D} into independent batches $\mathbf{B}_1, \dots, \mathbf{B}_K$, such that iterating DFW on \mathbf{B}_k , $k \in [K]$ yields with probability greater than $1 - \delta$:*

$$\text{dist}(\hat{\Phi}_K, \Phi_\star)^2 \leq \tilde{O} \left(C(\rho) \sigma_{\text{avg}}^2 \frac{(d_x r + \log(1/\delta))}{NT} \right), \quad (12)$$

where $C(\rho) > 0$ is a constant depending on the contraction rate ρ .

We note that the RHS of (12) has the “correct” scaling: noise level $\sigma_w^{(t)2}$ multiplied by # parameters of the representation, divided by the total amount of data NT . In particular, given a fine-tuning dataset of size N' sampled from a task $T + 1$ that shares the representation Φ_\star , computing the least squares weights $\hat{F}^{(T+1)}$ conditioned on $\hat{\Phi}_K$ yields a high-probability bound (cf. Appendix A.4.1) on

the parameter error

$$\begin{aligned} \left\| \hat{F}^{(T+1)} \hat{\Phi}_K - M_\star^{(T+1)} \right\|_F^2 &\lesssim \text{dist}(\hat{\Phi}_K, \Phi_\star)^2 + \sigma_w^{(T+1)2} \frac{d_y r + \log(1/\delta)}{N'} \\ &\lesssim C(\rho) \frac{\sigma_{\text{avg}}^2 (d_x r + \log(1/\delta))}{NT} + \frac{\sigma_w^{(T+1)2} (d_y r + \log(1/\delta))}{N'}, \end{aligned}$$

where we omit task-related quantities for clarity. We note that the above parameter recovery bound mirrors that of ERM estimates [Du et al., 2020, Zhang et al., 2023], where we note the latter fine-tuning term scales with $d_y r$ (the number of parameters in $F^{(T+1)}$) as opposed to r in the linear regression setting ($d_y = 1$).

4 Numerical Validation

We present numerical experiments to demonstrate the key importance of aspects of our proposed algorithm. We consider two scenarios: 1. linear regression with non-isotropic *iid* data, and 2. linear system identification. The linear regression experiments highlight the breakdown of standard approaches when approached with mildly non-isotropic data, thus highlighting the necessity of our proposed **De-biasing & Feature-whitening** steps, and our system identification experiments demonstrate the applicability of our algorithm to sequentially dependent (non-isotropic) data. Additional experiments and experiment details can be found in Appendix C.

4.1 Linear Regression with IID and Non-isotropic Data

We consider the observation model from (1), where we set the operator dimensions and rank as $d_x = d_y = 50$ and $r = 7$. We generate the T operators using the following steps: 1. a ground truth representation $\Phi_\star \in \mathbb{R}^{r \times d_x}$ is randomly generated through applying `thin_svd` to a random matrix with values $\overset{\text{i.i.d.}}{\sim} \mathcal{N}(0, 1)$, 2. a nominal task weight matrix $F_0 \in \mathbb{R}^{d_y \times r}$ is generated with elements $\overset{\text{i.i.d.}}{\sim} \mathcal{N}(0, 1)$, 3. task-specific weights $F_\star^{(t)} \in \mathbb{R}^{d_y \times r}$, $t \in [T]$ are generated by applying random rotations to F_0 . A non-isotropic covariance matrix Σ_x shared across all tasks is generated as $\Sigma_x = \frac{d_x \tilde{\Sigma}_x}{\text{Tr}(\tilde{\Sigma}_x)}$, where $\tilde{\Sigma}_x = \frac{1}{2}(U + U^\top)$, $U = 5 \cdot I_{d_x} + V$, with $V_{i,j} \overset{\text{i.i.d.}}{\sim} \text{Unif}(0, 1)$. We note that by design of U , Σ_x is only mildly non-isotropic. Figure 1a compares the performance of Algorithm 1, for a single-task ($T = 1$) and multiple tasks ($T = 25$), as well as standard alternating minimization-descent like **FedRep** [Collins et al., 2021] with $T = 25$. For each optimization iteration, we sample $N = 100$ fresh data per task. The figure highlights that **DFW** is able to make use of all source data to decrease variance and learn a representation to near-optimality. As predicted in §3.1, Figure 1a also shows that vanilla alternating minimization-descent is not able to improve beyond a highly suboptimal bias, despite all tasks sharing the same, rather mildly non-isotropic covariate distribution.

For a second experiment, we consider instead of applying vanilla alternating minimization-descent on a linear representation, we parameterize the representation by a neural network. In particular, we consider a ReLU-activated network with one hidden layer of dimension 64. We keep the same data-generation, with $N = 100$ fresh samples per optimization iteration per task, and compare **DFW** (on a linear representation) to **AMD** on the neural net representation. Since the subspace distance is no longer defined for the neural net representation, we measure optimality of the learned representations by computing the average least-squares loss with respect to a validation set generated through the nominal weight matrix F_0 . We plot the ‘‘optimal’’ loss as that attained by the ground truth operator $F_0 \Phi_\star$. We see in Figure 1b that, despite the much greater feature representation

power of the neural net, alternating minimization-descent plateaus for many iterations just like the linear case before finding a non-linear parameter representation that allows descent to optimality, taking almost two orders of magnitude more iterations than DFW to reach optimality. This feature learning phase is only exacerbated when there are fewer tasks. We note that in such a streaming data setting, the high iteration complexity of AMD translates to a greatly hampered sample-efficiency compared to DFW.

4.2 Linear System Identification

We consider a discrete-time linear system identification (sysID) problem, with dynamics

$$x_{i+1} = Ax_i + Bu_i + w_i, \quad i = 0, \dots, N - 1,$$

where x_i is the state of the system and u_i is the control input. In contrast to the previous example, the covariates are now additionally non-iid due to correlation over time. In particular, we can instantiate multi-task linear sysID in the form of (1),

$$x_{i+1}^{(t)} = M_\star^{(t)} z_i^{(t)} + w_i^{(t)}, \quad i = 0, \dots, N - 1$$

where $M_\star^{(t)} := [A^{(t)} \ B^{(t)}] = F^{(t)} \Phi_\star \in \mathbb{R}^{d_x \times d_z}$. The state-action pair at time instant i for all tasks $t \in [T]$ is embedded as $z_i^{(t)} = [x_i^{(t)\top} \ u_i^{(t)\top}]^\top$. The process noise $w_i^{(t)}$ and control action $u_i^{(t)}$ are assumed to be drawn from Gaussian distributions $\mathcal{N}(0, \Sigma_w)$ and $\mathcal{N}(0, \sigma_u^2 I_{d_u})$, respectively, where d_u represents the dimension of the control action. We set the state dimension $d_x = 25$, control dimension $d_u = 2$, latent dimension $r = 6$, horizon $N = 100$, and input variance $\sigma_u^2 = 1$. The generation process of the ground truth system matrices $M_\star^{(t)}$ follows a similar approach as described in the linear regression problem, with the addition of a normalization step of the nominal weight matrix F_0 to ensure system stability for all tasks $t \in [T]$. Furthermore, the process noise covariance Σ_w is parameterized in a similar manner as in the linear regression example, with $U = 5 \cdot I_{d_x} + 2 \cdot V$. The initial state $x_0^{(t)}$ is drawn iid across tasks from the system’s stationary distribution $\mathcal{N}(0, \Sigma_x^{(t)})$, which is determined by the solution to the discrete Lyapunov equation $\Sigma_x^{(t)} = A^{(t)} \Sigma_x^{(t)} (A^{(t)})^\top + \sigma_u^2 B^{(t)} (B^{(t)})^\top + \Sigma_w$. We note this implies the covariates $x_i^{(t)}$ are inherently non-isotropic and non-identically distributed across tasks. Figure 1c again demonstrates the advantage of leveraging multi-task data to reduce the error in computing a shared representation across the system matrices $M_\star^{(t)}$. In line with our theoretical findings, DFW continues to benefit from multiple tasks, even when the data is sequentially dependent. We see that FedRep remains suboptimal in this non-iid, non-isotropic setting.

5 Discussion and Future Work

We propose an efficient algorithm to provably recover linear operators across multiple tasks to optimality from non-iid non-isotropic data, recovering near oracle empirical risk minimization rates. We show that the benefit of learning over multiple tasks manifests in a lower noise level in the optimization and smaller sample requirements for individual tasks. These results contribute toward a general understanding of representation learning from an algorithmic and statistical perspective. Some immediate open questions are: whether good initialization of the representation is necessary, and whether the convergence rate of DFW can be optimized e.g., through ℓ^2 -regularized weights $\hat{F}^{(t)}$. Resolving these questions has important implications for the natural extension of our framework: as

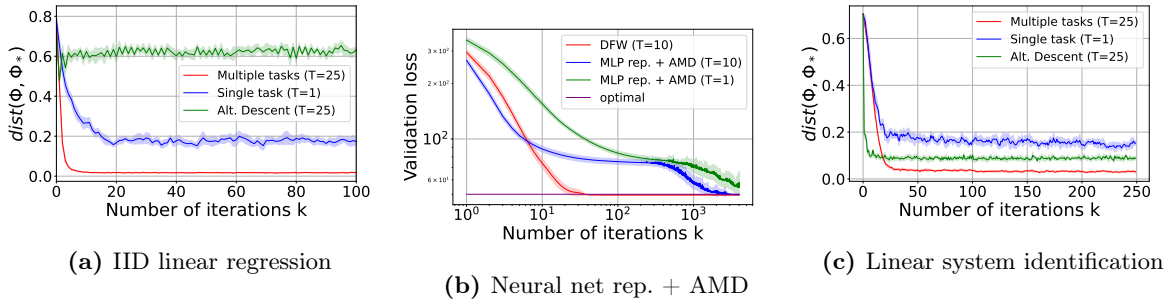


Figure 1: We plot the suboptimality the current and ground truth representation with respect to the number of iterations, comparing between the single and multiple-task settings of Algorithm 1 and the multi-task alternating minimization-descent. We observe performance improvement and variance reduction for multi-task DFW as predicted. All curves are are plotted as the mean with 95% confidence regions shaded

emphasized in [Collins et al., 2021], the alternating empirical risk minimization (holding representation fixed) and gradient descent (holding task-specific weights fixed) framework naturally extends to the nonlinear setting. Providing guarantees for nonlinear function classes is an exciting and impactful avenue for future work, which concurrent work is moving toward, e.g. for 2-layer ReLU networks [Collins et al., 2023] and kernel ridge regression [Meunier et al., 2023]. It remains to be seen whether a computationally-efficient algorithm can be established for nonlinear meta-learning in the non-iid and non-isotropic data regime, while preserving joint scaling in number of tasks and data.

References

- Liam Collins, Hamed Hassani, Aryan Mokhtari, and Sanjay Shakkottai. Exploiting shared representations for personalized federated learning. In *International Conference on Machine Learning*, pages 2089–2099. PMLR, 2021.
- Syedehsara Nayer and Namrata Vaswani. Fast and sample-efficient federated low rank matrix recovery from column-wise linear and quadratic projections. *IEEE Transactions on Information Theory*, 69(2):1177–1202, 2022.
- Brian Bullins, Elad Hazan, Adam Kalai, and Roi Livni. Generalize across tasks: Efficient algorithms for linear representation learning. In *algorithmic learning theory*, pages 235–246. PMLR, 2019.
- Simon S Du, Wei Hu, Sham M Kakade, Jason D Lee, and Qi Lei. Few-shot learning via learning the representation, provably. *arXiv preprint arXiv:2002.09434*, 2020.
- Nilesh Tripuraneni, Chi Jin, and Michael Jordan. Provable meta-learning of linear representations. In *International Conference on Machine Learning*, pages 10434–10443. PMLR, 2021.
- Kiran Koshy Thekumparampil, Prateek Jain, Praneeth Netrapalli, and Sewoong Oh. Sample efficient linear meta-learning by alternating minimization, 2021.
- Nikunj Saunshi, Arushi Gupta, and Wei Hu. A representation learning perspective on the importance of train-validation splitting in meta-learning, 2021.
- Aditya Modi, Mohamad Kazem Shirani Faradonbeh, Ambuj Tewari, and George Michailidis. Joint learning of linear time-invariant dynamical systems. *arXiv preprint arXiv:2112.10955*, 2021.

- Yiting Chen, Ana M Ospina, Fabio Pasqualetti, and Emiliano Dall’Anese. Multi-task system identification of similar linear time-invariant dynamical systems. *arXiv preprint arXiv:2301.01430*, 2023.
- Thomas T Zhang, Katie Kang, Bruce D Lee, Claire Tomlin, Sergey Levine, Stephen Tu, and Nikolai Matni. Multi-task imitation learning for linear dynamical systems. In *Learning for Dynamics and Control Conference*, pages 586–599. PMLR, 2023.
- Andreas Maurer, Massimiliano Pontil, and Bernardino Romera-Paredes. The benefit of multitask representation learning. *Journal of Machine Learning Research*, 17(81):1–32, 2016.
- Yee Whye Teh, Victor Bapst, Wojciech Marian Czarnecki, John Quan, James Kirkpatrick, Raia Hadsell, Nicolas Heess, and Razvan Pascanu. Distral: Robust multitask reinforcement learning, 2017.
- Matteo Hessel, Hubert Soyer, Lasse Espeholt, Wojciech Czarnecki, Simon Schmitt, and Hado van Hasselt. Multi-task deep reinforcement learning with popart, 2018.
- Avi Singh, Eric Jang, Alexander Irpan, Daniel Kappler, Murtaza Dalal, Sergey Levine, Mohi Khansari, and Chelsea Finn. Scalable multi-task imitation learning with autonomous improvement, 2020.
- Marc Peter Deisenroth, Peter Englert, Jan Peters, and Dieter Fox. Multi-task policy search for robotics. In *2014 IEEE International Conference on Robotics and Automation (ICRA)*, pages 3876–3881, 2014. doi: 10.1109/ICRA.2014.6907421.
- Rui Lu, Gao Huang, and Simon S. Du. On the power of multitask representation learning in linear mdp, 2021.
- Yuan Cheng, Songtao Feng, Jing Yang, Hong Zhang, and Yingbin Liang. Provable benefit of multitask representation learning in reinforcement learning, 2022.
- Andreas Maurer, Massimiliano Pontil, and Bernardino Romera-Paredes. The benefit of multitask representation learning, 2015.
- James Harrison, Apoorva Sharma, Roberto Calandra, and Marco Pavone. Control adaptation via meta-learning dynamics. In *Workshop on Meta-Learning at NeurIPS*, volume 2018, 2018.
- Spencer M Richards, Navid Azizan, Jean-Jacques Slotine, and Marco Pavone. Adaptive-control-oriented meta-learning for nonlinear systems. *arXiv preprint arXiv:2103.04490*, 2021.
- Guanya Shi, Kamyar Azizzadenesheli, Michael O’Connell, Soon-Jo Chung, and Yisong Yue. Meta-adaptive nonlinear control: Theory and algorithms. *Advances in Neural Information Processing Systems*, 34:10013–10025, 2021.
- Deepan Muthirayan, Dileep Kalathil, and Pramod P Khargonekar. Meta-learning online control for linear dynamical systems. *arXiv preprint arXiv:2208.10259*, 2022.
- Taosha Guo, Abed AlRahman Al Makdah, Vishaal Krishnan, and Fabio Pasqualetti. Imitation and transfer learning for lqg control. *arXiv preprint arXiv:2303.09002*, 2023.
- Lidong Li, Claudio De Persis, Pietro Tesi, and Nima Monshizadeh. Data-based transfer stabilization in linear systems. *arXiv preprint arXiv:2211.05536*, 2022.

- Han Wang, Leonardo F Toso, and James Anderson. Fedsysid: A federated approach to sample-efficient system identification. *arXiv preprint arXiv:2211.14393*, 2022.
- Lei Xin, Lintao Ye, George Chiu, and Shreyas Sundaram. Learning dynamical systems by leveraging data from similar systems. *arXiv preprint arXiv:2302.04344*, 2023.
- Mohamad Kazem Shirani Faradonbeh and Aditya Modi. Joint learning-based stabilization of multiple unknown linear systems. *IFAC-PapersOnLine*, 55(12):723–728, 2022.
- Gilbert W Stewart and Ji-guang Sun. *Matrix perturbation theory*. Academic press, 1990.
- Kaare Brandt Petersen, Michael Syskind Pedersen, et al. The matrix cookbook. *Technical University of Denmark*, 7(15):510, 2008.
- Lloyd N Trefethen and David Bau. *Numerical linear algebra*, volume 181. Siam, 2022.
- Yann LeCun, Léon Bottou, Genevieve B Orr, and Klaus-Robert Müller. Efficient backprop. In *Neural networks: Tricks of the trade*, pages 9–50. Springer, 2002.
- Suhas Kowshik, Dheeraj Nagaraj, Prateek Jain, and Praneeth Netrapalli. Near-optimal offline and streaming algorithms for learning non-linear dynamical systems. *Advances in Neural Information Processing Systems*, 34:8518–8531, 2021.
- Maryam Fazel, Rong Ge, Sham Kakade, and Mehran Mesbahi. Global convergence of policy gradient methods for the linear quadratic regulator. In *International Conference on Machine Learning*, pages 1467–1476. PMLR, 2018.
- Yasin Abbasi-Yadkori, Dávid Pál, and Csaba Szepesvári. Online least squares estimation with self-normalized processes: An application to bandit problems. *arXiv preprint arXiv:1102.2670*, 2011.
- Yasin Abbasi-Yadkori. Online learning for linearly parametrized control problems. 2013.
- Daniel Hsu, Sham M Kakade, and Tong Zhang. Random design analysis of ridge regression. In *Conference on learning theory*, pages 9–1. JMLR Workshop and Conference Proceedings, 2012.
- Joel A. Tropp. User-friendly tail bounds for sums of random matrices. *Foundations of Computational Mathematics*, 12(4):389–434, aug 2011. doi: 10.1007/s10208-011-9099-z. URL <https://doi.org/10.1007%2Fs10208-011-9099-z>.
- Liam Collins, Hamed Hassani, Mahdi Soltanolkotabi, Aryan Mokhtari, and Sanjay Shakkottai. Provable multi-task representation learning by two-layer relu neural networks. *arXiv preprint arXiv:2307.06887*, 2023.
- Dimitri Meunier, Zhu Li, Arthur Gretton, and Samory Kpotufe. Nonlinear meta-learning can guarantee faster rates. *arXiv preprint arXiv:2307.10870*, 2023.
- Tuhin Sarkar, Alexander Rakhlin, and Munther A Dahleh. Finite time lti system identification. *The Journal of Machine Learning Research*, 22(1):1186–1246, 2021.
- Vitaly Kuznetsov and Mehryar Mohri. Generalization bounds for non-stationary mixing processes. *Machine Learning*, 106(1):93–117, 2017.

- Stephen Tu and Benjamin Recht. Least-squares temporal difference learning for the linear quadratic regulator. In *International Conference on Machine Learning*, pages 5005–5014. PMLR, 2018.
- Roger A Horn and Charles R Johnson. *Matrix analysis*. Cambridge university press, 2012.
- Bin Yu. Rates of convergence for empirical processes of stationary mixing sequences. *The Annals of Probability*, pages 94–116, 1994.
- Bin Hu, Kaiqing Zhang, Na Li, Mehran Mesbahi, Maryam Fazel, and Tamer Başar. Toward a theoretical foundation of policy optimization for learning control policies. *Annual Review of Control, Robotics, and Autonomous Systems*, 6:123–158, 2023.
- Karl Krauth, Stephen Tu, and Benjamin Recht. Finite-time analysis of approximate policy iteration for the linear quadratic regulator. *Advances in Neural Information Processing Systems*, 32, 2019.
- Stephen Tu and Benjamin Recht. The gap between model-based and model-free methods on the linear quadratic regulator: An asymptotic viewpoint. In *Conference on Learning Theory*, pages 3036–3083. PMLR, 2019.
- Benjamin Recht. A tour of reinforcement learning: The view from continuous control. *Annual Review of Control, Robotics, and Autonomous Systems*, 2:253–279, 2019.
- Max Simchowitz and Dylan Foster. Naive exploration is optimal for online lqr. In *International Conference on Machine Learning*, pages 8937–8948. PMLR, 2020.
- Sarah Dean, Horia Mania, Nikolai Matni, Benjamin Recht, and Stephen Tu. Regret bounds for robust adaptive control of the linear quadratic regulator. *Advances in Neural Information Processing Systems*, 31, 2018.
- Sarah Dean, Horia Mania, Nikolai Matni, Benjamin Recht, and Stephen Tu. On the sample complexity of the linear quadratic regulator. *Foundations of Computational Mathematics*, 20(4): 633–679, 2020.
- Naman Agarwal, Elad Hazan, and Karan Singh. Logarithmic regret for online control. *Advances in Neural Information Processing Systems*, 32, 2019a.
- Naman Agarwal, Brian Bullins, Elad Hazan, Sham Kakade, and Karan Singh. Online control with adversarial disturbances. In *International Conference on Machine Learning*, pages 111–119. PMLR, 2019b.
- Ingvar Ziemann, Anastasios Tsiamis, Henrik Sandberg, and Nikolai Matni. How are policy gradient methods affected by the limits of control? In *2022 IEEE 61st Conference on Decision and Control (CDC)*, pages 5992–5999. IEEE, 2022.
- Ingvar Ziemann and Henrik Sandberg. Regret lower bounds for learning linear quadratic gaussian systems. *arXiv preprint arXiv:2201.01680*, 2022.
- Bruce D Lee, Ingvar Ziemann, Anastasios Tsiamis, Henrik Sandberg, and Nikolai Matni. The fundamental limitations of learning linear-quadratic regulators. *arXiv preprint arXiv:2303.15637*, 2023.
- Max Simchowitz, Horia Mania, Stephen Tu, Michael I Jordan, and Benjamin Recht. Learning without mixing: Towards a sharp analysis of linear system identification. In *Conference On Learning Theory*, pages 439–473. PMLR, 2018.

Anastasios Tsiamis, Ingvar M Ziemann, Manfred Morari, Nikolai Matni, and George J Pappas. Learning to control linear systems can be hard. In *Conference on Learning Theory*, pages 3820–3857. PMLR, 2022.

Yassir Jedra and Alexandre Proutiere. Finite-time identification of stable linear systems optimality of the least-squares estimator. In *2020 59th IEEE Conference on Decision and Control (CDC)*, pages 996–1001, 2020. doi: 10.1109/CDC42340.2020.9304362.

Stephen Tu, Roy Frostig, and Mahdi Soltanolkotabi. Learning from many trajectories. *arXiv preprint arXiv:2203.17193*, 2022.

Alexander Goldenshluger and Assaf Zeevi. Nonasymptotic bounds for autoregressive time series modeling. *The Annals of Statistics*, 29(2):417–444, 2001.

Contents

1	Introduction	1
1.1	Related Work	3
2	Problem Formulation	3
3	Sample-Efficient Linear Representation Learning	5
3.1	Perils of (Vanilla) Gradient Descent on the Representation	5
3.2	A Task-Efficient Algorithm: De-bias & Feature-whiten	6
3.3	Algorithm Guarantees	8
4	Numerical Validation	12
4.1	Linear Regression with IID and Non-isotropic Data	12
4.2	Linear System Identification	13
5	Discussion and Future Work	13
A	Theoretical Analysis of DFW (Algorithm 1)	20
A.1	Preliminaries	20
A.2	The IID Setting	23
A.3	The Non-IID Setting	35
A.4	Converting to Sample Complexity Bounds	36
A.4.1	Near-ERM Transfer Learning	37
B	Case Study: Linear Dynamical Systems	38
B.1	Linear System Identification	38
B.2	Imitation Learning	40
C	Additional Numerical Experiments and Details	41
C.1	Linear Regression with IID and Non-isotropic Data	42
C.2	System Identification	43
C.3	Imitation Learning	44

A Theoretical Analysis of DFW (Algorithm 1)

A.1 Preliminaries

We introduce some preliminary concepts and results that recur throughout our analysis. A fundamental concept in the analysis of least-squares solutions is the self-normalized martingale [Abbasi-Yadkori et al., 2011, Abbasi-Yadkori, 2013].

Lemma A.1 (cf. Zhang et al. [2023, Lemma B.3]) *Let $\{x_i\}_{i \geq 1}$ be a \mathbb{R}^{d_x} -valued process adapted to a filtration $\{\mathcal{F}_i\}_{i \geq 1}$. Let $\{w_i\}_{i \geq 1}$ be a \mathbb{R}^{d_y} -valued process adapted to $\{\mathcal{F}_i\}_{i \geq 2}$. Suppose that $\{w_i\}_{i \geq 1}$ is a σ^2 -subgaussian martingale difference sequence, i.e.,:*

$$\mathbb{E}[w_i \mid \mathcal{F}_i] = 0, \quad (13)$$

$$\mathbb{E}[\exp(\lambda v^\top w_i) \mid \mathcal{F}_i] \leq \exp\left(\frac{\lambda^2 \sigma^2 \|v\|^2}{2}\right) \quad \forall \mathcal{F}_i\text{-measurable } \lambda \in \mathbb{R}, v \in \mathbb{R}^{d_y}. \quad (14)$$

For $\Lambda \in \mathbb{R}^{d_y \times d_x}$, let $\{M_k(\Lambda)\}_{k \geq 1}$ be the \mathbb{R} -valued process:

$$M_k(\Lambda) = \exp\left(\frac{1}{\sigma} \sum_{i=1}^k \langle \Lambda x_i, w_i \rangle - \frac{1}{2} \sum_{i=1}^k \|\Lambda x_i\|^2\right). \quad (15)$$

Then, the process $\{M_k(\Lambda)\}_{k \geq 1}$ satisfies $\mathbb{E}[M_k(\Lambda)] \leq 1$ for all $k \geq 1$.

In particular, this implies the following self-normalized martingale inequality that handles multiple matrix-valued self-normalized martingales simultaneously. This can be seen as an instantiation of the Hilbert space variant from Abbasi-Yadkori [2013].

Proposition A.1 (cf. Zhang et al. [2023, Prop. B.1], Sarkar et al. [2021, Proposition 8.2])

Fix $T \in \mathbb{N}_+$. For $t \in [T]$, let $\{x_i^{(t)}, w_i^{(t)}\}_{i \geq 1}$ be a $\mathbb{R}^{d_x} \times \mathbb{R}^{d_y}$ -valued process and $\{\mathcal{F}_i^{(t)}\}_{i \geq 1}$ be a filtration such that $\{x_i^{(t)}\}_{i \geq 1}$ is adapted to $\{\mathcal{F}_i^{(t)}\}_{i \geq 1}$, $\{w_i^{(t)}\}_{i \geq 1}$ is adapted to $\{\mathcal{F}_i^{(t)}\}_{i \geq 2}$, and $\{w_i^{(t)}\}_{i \geq 1}$ is a σ^2 -subgaussian martingale difference sequence. Suppose that for all $t_1 \neq t_2$, the process $\{x_i^{(t_1)}, w_i^{(t_1)}\}$ is independent of $\{x_i^{(t_2)}, w_i^{(t_2)}\}$. Fix (non-random) positive definite matrices $\{V^{(t)}\}_{t=1}^T$. For $k \geq 1$ and $t \in [T]$, define $\hat{\Sigma}_k^{(t)} := \sum_{i=1}^k x_i x_i^\top$. Then, given any fixed $N, T \in \mathbb{N}_+$, with probability at least $1 - \delta$:

$$\sum_{t=1}^T \left\| \sum_{i=1}^N w_i^{(t)} x_i^{(t)\top} \left(V^{(t)} + \hat{\Sigma}_N^{(t)}\right)^{-1/2} \right\|_F^2 \leq d_y \sigma^2 \sum_{t=1}^T \log\left(\frac{\det(V^{(t)} + \hat{\Sigma}_N^{(t)})}{\det(V^{(t)})}\right) + 2\sigma^2 \log(1/\delta) \quad (16)$$

Alternatively, in the spectral norm, we have with probability at least $1 - \delta$,

$$\begin{aligned} \sum_{t=1}^T \left\| \sum_{i=1}^N w_i^{(t)} x_i^{(t)\top} \left(V^{(t)} + \hat{\Sigma}_N^{(t)}\right)^{-1/2} \right\|_2^2 &\leq 4\sigma^2 \sum_{t=1}^T \log\left(\frac{\det(V^{(t)} + \hat{\Sigma}_N^{(t)})}{\det(V^{(t)})}\right) \\ &+ 13d_y T \sigma^2 + 8\sigma^2 \log(1/\delta). \end{aligned} \quad (17)$$

We note that the above bound also holds for individual tasks $t \in [T]$ simply by removing the summand over t . We introduce the following useful two-sided concentration inequality for the sample covariance of iid subgaussian covariates.

Lemma A.2 (Du et al. [2020, Claim A.1, A.2]) Let $x_1, \dots, x_N \in \mathbb{R}^d$ be iid random vectors that satisfy $\mathbb{E}[x_i] = 0$, $\mathbb{E}[x_i x_i^\top] = \Sigma$, and x_i is γ^2 -subgaussian. Fix $\delta \in (0, 1)$. Suppose $N \gtrsim \gamma^4(d + \log(1/\delta))$. Then with probability at least $1 - \delta$, the following holds

$$0.9\Sigma \preceq \frac{1}{N} \sum_{i=1}^N x_i x_i^\top \preceq 1.1\Sigma. \quad (18)$$

Furthermore, for any matrix $U \in \mathbb{R}^{r \times d_x}$, as long as $N \gtrsim \gamma^4(r + \log(1/\delta))$, we have with probability at least $1 - \delta$

$$0.9U\Sigma U^\top \preceq \frac{1}{N} \sum_{i=1}^N U x_i x_i^\top U^\top \preceq 1.1U\Sigma U^\top. \quad (19)$$

Combining Proposition A.1 and Lemma A.2 yields the following self-normalized martingale bound without the non-random lower bound $V^{(t)}$.

Lemma A.3 Consider the quantities defined in Proposition A.1 and assume $x_i^{(t)}$ are zero-mean and γ^2 -subgaussian. Then, as long as $N \gtrsim \gamma^4(d_x + \log(T/\delta))$, with probability at least $1 - \delta$:

$$\begin{aligned} \sum_{t=1}^T \left\| \sum_{i=1}^N w_i^{(t)} x_i^{(t)\top} \left(\hat{\Sigma}_N^{(t)} \right)^{-1/2} \right\|_F^2 &\leq 2d_y d_x T \sigma^2 + 4\sigma^2 \log(T/\delta), \text{ or} \\ \sum_{t=1}^T \left\| \sum_{i=1}^N w_i^{(t)} x_i^{(t)\top} \left(\hat{\Sigma}_N^{(t)} \right)^{-1/2} \right\|_2^2 &\leq 8d_x T \sigma^2 + 26d_y T \sigma^2 + 16\sigma^2 \log(T/\delta). \end{aligned}$$

Proof: we observe that if $\hat{\Sigma}_N^{(t)} \succeq V^{(t)}$, then

$$2\hat{\Sigma}_N^{(t)} \succeq V^{(t)} + \hat{\Sigma}_N^{(t)} \implies \left(\hat{\Sigma}_N^{(t)} \right)^{-1} \preceq 2 \left(V^{(t)} + \hat{\Sigma}_N^{(t)} \right)^{-1}.$$

This implies

$$\begin{aligned} &\sum_{t=1}^T \mathbf{1} \left\{ \hat{\Sigma}_N^{(t)} \succeq V^{(t)} \right\} \left\| \sum_{i=1}^N w_i^{(t)} x_i^{(t)\top} \left(\hat{\Sigma}_N^{(t)} \right)^{-1/2} \right\|_F^2 \\ &\leq 2 \sum_{t=1}^T \mathbf{1} \left\{ \hat{\Sigma}_N^{(t)} \succeq V^{(t)} \right\} \left\| \sum_{i=1}^N w_i^{(t)} x_i^{(t)\top} \left(V^{(t)} + \hat{\Sigma}_N^{(t)} \right)^{-1/2} \right\|_F^2. \end{aligned}$$

Defining $\Sigma^{(t)} := \mathbb{E} \left[x_i^{(t)} x_i^{(t)\top} \right]$, let us consider for each t the event:

$$0.9\Sigma^{(t)} \preceq \hat{\Sigma}_N^{(t)} \preceq 1.1\Sigma^{(t)},$$

which by Lemma A.2 occurs with probability at least $1 - \delta$ as long as $N \gtrsim \gamma^4(d_x + \log(1/\delta))$. Setting $V^{(t)} := 0.9N\Sigma^{(t)}$ and conditioning on the above event, we observe that by definition $\hat{\Sigma}_N^{(t)} \succeq V^{(t)}$, and

$$\begin{aligned} \log \left(\frac{\det \left(V^{(t)} + \hat{\Sigma}_N^{(t)} \right)}{\det(V^{(t)})} \right) &= \log \det \left(I_{d_x} + \hat{\Sigma}_N^{(t)} \left(V^{(t)} \right)^{-1} \right) \\ &= \log \det \left(\left(1 + \frac{1.1}{0.9} \right) I_{d_x} \right) \\ &\leq d_x. \end{aligned}$$

Plugging this into Proposition A.1 and union-bounding over the desirable event over each $t \in [T]$, and adjusting the failure probability $\delta/T \mapsto \delta$, we get our desired result. \blacksquare

In order to instantiate our bounds for non-iid covariates, we introduce the notions of β -mixing stationary processes [Kuznetsov and Mohri, 2017, Tu and Recht, 2018].

Definition A.1 (β -mixing) Let $\{x_i\}_{t \geq 1}$ be a \mathbb{R}^d -valued discrete-time stochastic process adapted to filtration $\{\mathcal{F}_i\}_{t=1}^\infty$. We denote the stationary distribution ν_∞ . We define the β -mixing coefficient

$$\beta(k) := \sup_{t \geq 1} \mathbb{E}_{\{x_\ell\}_{\ell=1}^t} \left[\left\| \mathbb{P}_{x_{t+k}}(\cdot \mid \mathcal{F}_t) - \nu_\infty \right\|_{\text{tv}} \right], \quad (20)$$

where $\|\cdot\|_{\text{tv}}$ denotes the total variation distance between probability measures.

Intuitively, the β -mixing coefficient measures how quickly on average a process mixes to the stationary distribution along any sample path. To see how β -mixing is instantiated, let $\{x_i\}_{t=1}^T$ be a sample path from a β -mixing process. Consider the following subsampled paths formed by taking every a -th covariate of $\{x_i\}$:

$$X_{(j)}^T := \{x_i : 1 \leq t \leq T, (t-1 \bmod a) = j-1\}, \quad j = 1, \dots, a. \quad (21)$$

Let the integers m_1, \dots, m_a and index sets $I_{(1)}, \dots, I_{(a)}$ denote the sizes and indices of $X_{(1)}^T, \dots, X_{(a)}^T$, respectively. Finally, let $X_\infty^{m_j}$ denote a sequence of m_j iid draws from the stationary distribution ν_∞ . The following is a key lemma in relating a correlated process to iid draws.

Lemma A.4 (Kuznetsov and Mohri [2017, Proposition 2]) Let $g(\cdot)$ be a real-valued Borel-measurable function satisfying $-M_1 \leq g(\cdot) \leq M_2$ for some $M_1, M_2 \geq 0$. Then, for all $j = 1, \dots, a$.

$$\left| \mathbb{E}[g(X_\infty^{m_j})] - \mathbb{E}[g(X_{(j)}^T)] \right| \leq (M_1 + M_2)m_j\beta(a).$$

In our analysis, we often instantiate Lemma A.4 with $g(\cdot)$ as an indicator function on a success event. For appropriately selected block length a , we are thus able to relate simpler iid analysis on $X_\infty^{m_j}$ to the original process $X_{(j)}^T$, accruing an additional factor in the failure probability. Lastly, we introduce a standard matrix concentration inequality.

Lemma A.5 (Matrix Hoeffding [Tropp, 2011]) Let $\{X_t\}_{t=1}^T \subset \mathbb{R}^{d \times d}$ be a sequence of independent, random symmetric matrices, and let $\{B_t\}_{t=1}^T$ be a sequence of fixed symmetric matrices. Assume each random matrix satisfies

$$\mathbb{E}[X_t] = 0, \quad X_t^2 \preceq B_t^2 \text{ almost surely.}$$

Then for all $t \geq 0$,

$$\mathbb{P} \left[\lambda_{\max} \left(\sum_{t=1}^T X_t \right) \geq t \right] \leq d \cdot \exp \left(-\frac{t^2}{8\sigma^2} \right), \quad \sigma^2 := \left\| \sum_{t=1}^T B_t^2 \right\|.$$

In particular, for general rectangular $\{M_t\}_{t=1}^T \subset \mathbb{R}^{d_1 \times d_2}$, we may define $X_t := \begin{bmatrix} 0 & M_t \\ M_t^\top & 0 \end{bmatrix}$ to yield a singular value concentration inequality. Assume each M_t satisfies

$$\mathbb{E}[M_t] = 0, \quad X_t^2 \preceq B_t^2 \text{ almost surely.}$$

Then for all $t \geq 0$,

$$\mathbb{P} \left[\sigma_{\max} \left(\sum_{t=1}^T M_t \right) \geq t \right] \leq (d_1 + d_2) \cdot \exp \left(-\frac{t^2}{8\sigma^2} \right), \quad \sigma^2 := \left\| \sum_{t=1}^T B_t^2 \right\|.$$

As hinted by the indexing of the matrices, by leveraging the independence of processes across tasks t , Lemma A.5 can be used to bound various quantities averaged across tasks, under the important caveat that the matrices are *zero-mean*, which ties back to the necessity of our de-biasing and feature-whitening adjustments.

A.2 The IID Setting

We recall that given the current representation iterate $\hat{\Phi}$, an iid draw of a multitask dataset $\{(x_i^{(t)}, y_i^{(t)})\}_{t=1, i=1}^{T, N}$, $t = 1, \dots, T$, and DFW trajectory partitions $\mathcal{N}_1, \mathcal{N}_2$, the least squares weights $\hat{F}^{(t)}$ can be written as

$$\begin{aligned} \hat{F}^{(t)} &= \operatorname{argmin}_F \sum_{i \in \mathcal{N}_1} \left\| y_i^{(t)} - F z_i^{(t)} \right\|^2 \\ &= F_\star^{(t)} \Phi_\star X_{\mathcal{N}_1}^{(t)\top} Z_{\mathcal{N}_1}^{(t)} \left(\hat{\Sigma}_{z, \mathcal{N}_1}^{(t)} \right)^{-1} + W_{\mathcal{N}_1}^{(t)\top} Z_{\mathcal{N}_1}^{(t)} \left(\hat{\Sigma}_{z, \mathcal{N}_1}^{(t)} \right)^{-1} \\ &= F_\star^{(t)} \Phi_\star \hat{\Phi}^\top + F_\star^{(t)} \Phi_\star \left(I_{d_x} - \hat{\Phi}^\top \hat{\Phi} \right) X_{\mathcal{N}_1}^{(t)\top} Z_{\mathcal{N}_1}^{(t)} \left(\hat{\Sigma}_{z, \mathcal{N}_1}^{(t)} \right)^{-1} + W_{\mathcal{N}_1}^{(t)\top} Z_{\mathcal{N}_1}^{(t)} \left(\hat{\Sigma}_{z, \mathcal{N}_1}^{(t)} \right)^{-1}. \end{aligned} \quad (22)$$

Now recalling the DFW representation update in the iid setting (6), we have

$$R\hat{\Phi}_+ = \hat{\Phi} - \frac{\eta}{T} \sum_{t=1}^T \hat{F}^{(t)\top} \left(\hat{F}^{(t)} \hat{\Phi} - F_\star^{(t)} \Phi_\star \right) - \frac{\eta}{T} \sum_{t=1}^T \hat{F}^{(t)\top} W_{\mathcal{N}_2}^{(t)\top} X_{\mathcal{N}_2}^{(t)} \left(\hat{\Sigma}_x^{(t)} \right)^{-1}. \quad (23)$$

Right multiplying the update by $\Phi_{\star, \perp}^\top$, we get

$$\begin{aligned} R\hat{\Phi}_+ \Phi_{\star, \perp}^\top &= \hat{\Phi} \Phi_{\star, \perp}^\top - \frac{\eta}{T} \sum_{t=1}^T \hat{F}^{(t)\top} \left(\hat{F}^{(t)} \hat{\Phi} - F_\star^{(t)} \Phi_\star \right) \Phi_{\star, \perp}^\top - \frac{\eta}{T} \sum_{t=1}^T \hat{F}^{(t)\top} W_{\mathcal{N}_2}^{(t)\top} X_{\mathcal{N}_2}^{(t)} \left(\hat{\Sigma}_{x, \mathcal{N}_2}^{(t)} \right)^{-1} \Phi_{\star, \perp}^\top \\ &= \underbrace{\left(I_{d_x} - \frac{\eta}{T} \sum_{t=1}^T \hat{F}^{(t)\top} \hat{F}^{(t)} \right)}_{\text{"contraction" term}} \hat{\Phi} \Phi_{\star, \perp}^\top - \underbrace{\frac{\eta}{T} \sum_{t=1}^T \hat{F}^{(t)\top} W_{\mathcal{N}_2}^{(t)\top} X_{\mathcal{N}_2}^{(t)} \left(\hat{\Sigma}_{x, \mathcal{N}_2}^{(t)} \right)^{-1}}_{\text{"noise" term}} \Phi_{\star, \perp}^\top, \end{aligned}$$

where the last line is composed of a contraction term and a noise term. We start with an analysis of the noise term.

Bounding the noise term

We observe that since $\hat{F}^{(t)}$ is by construction independent of $W_{\mathcal{N}_2}^{(t)}, X_{\mathcal{N}_2}^{(t)}$, by the independence of $x_i^{(t)}$ across t and i , and the noise independence $w_i^{(t)} \perp x_i^{(t)}$, we find

$$\mathbb{E} \left[\frac{1}{T} \sum_{t=1}^T \hat{F}^{(t)\top} W_{\mathcal{N}_2}^{(t)\top} X_{\mathcal{N}_2}^{(t)} \left(\hat{\Sigma}_{x, \mathcal{N}_2}^{(t)} \right)^{-1} \right] = \frac{1}{T} \sum_{t=1}^T \mathbb{E} \left[\hat{F}^{(t)} \right]^\top \mathbb{E} \left[W_{\mathcal{N}_2}^{(t)} \right] \mathbb{E} \left[X_{\mathcal{N}_2}^{(t)} \left(\hat{\Sigma}_{x, \mathcal{N}_2}^{(t)} \right)^{-1} \right] = 0.$$

Therefore, we set up for an application of Lemma A.5. Toward doing so, we prove the following two ingredients: 1. a high probability bound on $\|\hat{F}^{(t)}\|$, 2. a high probability bound on the least-squares noise-esque term $\|\hat{F}^{(t)\top} W_{\mathcal{N}_2}^{(t)\top} X_{\mathcal{N}_2}^{(t)} \left(\hat{\Sigma}_{x, \mathcal{N}_2}^{(t)} \right)^{-1}\|$. We then condition on these two high-probability

events to instantiate the almost-sure boundedness in Lemma A.5. We start with the analysis of $\hat{F}^{(t)}$. By (22), we have

$$\left\| \hat{F}^{(t)} \right\| \leq \left\| F_\star^{(t)} \right\| + \left\| F_\star^{(t)} \right\| \left\| \Phi_\star \mathcal{P}_{\hat{\Phi}}^\perp X_{\mathcal{N}_1}^{(t)\top} Z_{\mathcal{N}_1}^{(t)} \left(\hat{\Sigma}_{z, \mathcal{N}_1}^{(t)} \right)^{-1} \right\| + \left\| W_{\mathcal{N}_1}^{(t)\top} Z_{\mathcal{N}_1}^{(t)} \left(\hat{\Sigma}_{z, \mathcal{N}_1}^{(t)} \right)^{-1} \right\|.$$

Lemma A.6 *Let $|\mathcal{N}_1| := N_1 \gtrsim \gamma^4 (r + \log(1/\delta))$. Then, with probability greater than $1 - \delta$, we have*

$$\left\| \Phi_\star \mathcal{P}_{\hat{\Phi}}^\perp X_{\mathcal{N}_1}^{(t)\top} Z_{\mathcal{N}_1}^{(t)} \left(\hat{\Sigma}_{z, \mathcal{N}_1}^{(t)} \right)^{-1} \right\| \leq \frac{5}{4} \text{dist}(\hat{\Phi}, \Phi_\star) \kappa \left(\Sigma_x^{(t)} \right), \quad (24)$$

$$\left\| W_{\mathcal{N}_1}^{(t)\top} Z_{\mathcal{N}_1}^{(t)} \left(\hat{\Sigma}_{z, \mathcal{N}_1}^{(t)} \right)^{-1} \right\| \lesssim \sigma_w^{(t)} \sqrt{\frac{d_y + r + \log(1/\delta)}{\lambda_{\min}(\Sigma_z^{(t)}) N_1}}. \quad (25)$$

Proof: we begin with the bound (24). We observe that by definition $\frac{1}{N_1} X_{\mathcal{N}_1}^{(t)\top} X_{\mathcal{N}_1}^{(t)} = \hat{\Sigma}_{x, \mathcal{N}_1}^{(t)}$, and $\Phi_\star \mathcal{P}_{\hat{\Phi}}^\perp, \hat{\Phi}$ are $r \times d_x$ matrices. Therefore, we invoke Lemma A.2 twice to find: as long as $N_1 \gtrsim \gamma^4 (r + \log(1/\delta))$, with probability at least $1 - \delta$, the following bounds hold simultaneously:

$$\begin{aligned} \frac{1}{N_1} \left\| \Phi_\star \mathcal{P}_{\hat{\Phi}}^\perp X_{\mathcal{N}_1}^{(t)\top} \right\|^2 &\leq 1.1 \left\| \Phi_\star \mathcal{P}_{\hat{\Phi}}^\perp \left(\Sigma_x^{(t)} \right)^{1/2} \right\|^2 \leq 1.1 \text{dist}(\hat{\Phi}, \Phi_\star)^2 \lambda_{\max} \left(\Sigma_x^{(t)} \right) \\ \frac{1}{N_1} \left\| Z_{\mathcal{N}_1}^{(t)} \right\|^2 &\leq 1.1 \left\| \Sigma_z^{(t)} \right\| \leq 1.1 \lambda_{\max} \left(\Sigma_x^{(t)} \right) \\ \left\| \left(\hat{\Sigma}_{z, \mathcal{N}_1}^{(t)} \right)^{-1} \right\| &\leq 0.9 \lambda_{\min}(\Sigma_z^{(t)})^{-1} \leq 0.9 \lambda_{\min}(\Sigma_x^{(t)})^{-1}, \end{aligned}$$

where we recall that $\Sigma_z^{(t)} = \hat{\Phi} \Sigma_x^{(t)} \hat{\Phi}^\top$. Therefore, applying Cauchy-Schwarz on the LHS of (24) and the above bounds (converting $1.1/0.9 < 5/4$) yields the desired upper bound on the RHS. Moving onto (25), we observe that since $\hat{\Phi}$ is fixed, $\{w_i^{(t)}, z_i^{(t)}\}_{i \geq 1}$ is an $\mathbb{R}^{d_y} \times \mathbb{R}^r$ -valued martingale difference sequence. Therefore, we may apply Lemma A.2 and Lemma A.3 to find: as long as $N_1 \gtrsim \gamma^4 (r + \log(1/\delta))$, with probability at least $1 - \delta$,

$$\begin{aligned} \left\| W_{\mathcal{N}_1}^{(t)\top} Z_{\mathcal{N}_1}^{(t)} \left(\hat{\Sigma}_{z, \mathcal{N}_1}^{(t)} \right)^{-1} \right\| &\leq \left\| W_{\mathcal{N}_1}^{(t)\top} Z_{\mathcal{N}_1}^{(t)} \left(\hat{\Sigma}_{z, \mathcal{N}_1}^{(t)} \right)^{-1/2} \right\| \lambda_{\min} \left(\hat{\Sigma}_{z, \mathcal{N}_1}^{(t)} \right)^{-1/2} \\ &\lesssim \sqrt{\frac{\sigma_w^{(t)2} (d_y + r + \log(1/\delta))}{\lambda_{\min}(\Sigma_x^{(t)}) N_1}}, \end{aligned}$$

which establishes the bound (25). ■

Therefore, by assuming $\text{dist}(\hat{\Phi}, \Phi_\star)$ is sufficiently small, and that N_1 is large enough to offset the noise bound (25), we immediately get the following bound relating $\|\hat{F}^{(t)}\|$ to $\|F_\star^{(t)}\|$.

Lemma A.7 *Assume*

$$N_1 \gtrsim \max \left\{ \gamma^4 (r + \log(1/\delta)), \frac{\sigma_w^{(t)2}}{C^2 \|F_\star^{(t)}\|^2 \lambda_{\min}(\Sigma_x^{(t)})} (d_y + r + \log(1/\delta)) \right\},$$

and $\text{dist}(\hat{\Phi}, \Phi_\star) \leq \frac{2}{5} C \kappa \left(\Sigma_x^{(t)} \right)^{-1}$, for fixed $C > 0$. Then with probability at least $1 - \delta$

$$\|\hat{F}^{(t)}\| \leq (1 + C) \|F_\star^{(t)}\|. \quad (26)$$

The factor $C > 0$ serves as a free parameter which we can determine later—a larger C implies a relaxed requirement on the initial condition (disappears when $C \geq \frac{5}{2}\kappa(\Sigma_x^{(t)})$) and burn-in requirement on N_1 , but results in a larger subgaussian-parameter bound on the representation update noise term (23), as we demonstrate: given that the success event of Lemma A.7 holds, then by the definition of subgaussianity (Assumption 3.1), we observe that $\hat{F}^{(t)\top} w_i^{(t)}$ is zero-mean and $(1+C)^2 \sigma_w^{(t)2} \|F_\star^{(t)}\|^2$ -subgaussian, supported on \mathbb{R}^r . Therefore, bounding

$$\left\| \hat{F}^{(t)\top} W_{\mathcal{N}_2}^{(t)\top} X_{\mathcal{N}_2}^{(t)} \left(\hat{\Sigma}_{x, \mathcal{N}_2}^{(t)} \right)^{-1} \right\| \leq \left\| \hat{F}^{(t)\top} W_{\mathcal{N}_2}^{(t)\top} X_{\mathcal{N}_2}^{(t)} \left(\hat{\Sigma}_{x, \mathcal{N}_2}^{(t)} \right)^{-1/2} \right\| \lambda_{\min}(\hat{\Sigma}_{x, \mathcal{N}_2}^{(t)})^{-1/2},$$

we invoke Proposition A.1 and Lemma A.2 to get the following bound.

Lemma A.8 *Let the conditions of Lemma A.7 hold. Then, for a fixed $t \in [T]$, as long as $|\mathcal{N}_2| := N_2 \gtrsim \gamma^4 (d_x + \log(1/\delta))$, with probability at least $1 - \delta$,*

$$\left\| \hat{F}^{(t)\top} W_{\mathcal{N}_2}^{(t)\top} X_{\mathcal{N}_2}^{(t)} \left(\hat{\Sigma}_{x, \mathcal{N}_2}^{(t)} \right)^{-1} \right\| \lesssim (1+C) \sigma_w^{(t)} \|F_\star^{(t)}\| \sqrt{\frac{d_x + \log(1/\delta)}{\lambda_{\min}(\Sigma_x^{(t)}) N_2}}. \quad (27)$$

With a bound on the task-specific noise term in hand, we may now produce the final bound on the (task-averaged) noise term.

Proposition A.2 (Noise term bound) *Assume*

$$N_1 \gtrsim \max \left\{ \gamma^4 (r + \log(T/\delta)), \max_t \frac{\sigma_w^{(t)2}}{C^2 \|F_\star^{(t)}\|^2 \lambda_{\min}(\Sigma_x^{(t)})} (d_y + r + \log(T/\delta)) \right\},$$

$$N_2 \gtrsim \gamma^4 (d_x + \log(T/\delta)),$$

and $\text{dist}(\hat{\Phi}, \Phi_\star) \leq \max_t \frac{2}{5} C \kappa(\Sigma_x^{(t)})^{-1}$, for fixed $C > 0$. Then, with probability at least $1 - \delta$,

$$\left\| \frac{1}{T} \sum_{t=1}^T \hat{F}^{(t)\top} W_{\mathcal{N}_2}^{(t)\top} X_{\mathcal{N}_2}^{(t)} \left(\hat{\Sigma}_{x, \mathcal{N}_2}^{(t)} \right)^{-1} \right\| \lesssim \sigma_{\text{avg}} (1+C) \sqrt{\frac{d_x + \log(T/\delta)}{T N_2} \log\left(\frac{d_x}{\delta}\right)},$$

where $\sigma_{\text{avg}} := \sqrt{\frac{1}{T} \sum_{t=1}^T \frac{\sigma_w^{(t)2} \|F_\star^{(t)}\|^2}{\lambda_{\min}(\Sigma_x^{(t)})}}$ is the task-averaged noise-level.

Proof of Proposition A.2: we set up for an application of the Matrix Hoeffding bound (Lemma A.5). By union bounding over the task-specific noise bound Lemma A.8, we have with probability at least $1 - \delta$, for all $t \in [T]$ simultaneously:

$$\left\| \hat{F}^{(t)\top} W_{\mathcal{N}_2}^{(t)\top} X_{\mathcal{N}_2}^{(t)} \left(\hat{\Sigma}_{x, \mathcal{N}_2}^{(t)} \right)^{-1} \right\| \lesssim (1+C) \frac{\sigma_w^{(t)} \|F_\star^{(t)}\|}{\sqrt{\lambda_{\min}(\Sigma_x^{(t)})}} \sqrt{\frac{d_x + \log(T/\delta)}{N_2}},$$

given the assumed burn-in conditions hold. Therefore, by setting

$$B^{(t)} = \mathcal{O}(1) \frac{\sigma_w^{(t)} \|F_\star^{(t)}\|}{\sqrt{\lambda_{\min}(\Sigma_x^{(t)})}} \sqrt{\frac{d_x + \log(T/\delta)}{N_2}} I_{d_x+r}$$

$$\sigma^2 = \left\| \sum_{t=1}^T (B^{(t)})^2 \right\| = \left(\sum_{t=1}^T \frac{\sigma_w^{(t)2} \|F_\star^{(t)}\|^2}{\lambda_{\min}(\Sigma_x^{(t)})} \right) (1+C)^2 \frac{d_x + \log(T/\delta)}{N_2}$$

$$= T \sigma_{\text{avg}}^2 (1+C)^2 \frac{d_x + \log(T/\delta)}{N_2}$$

we invoke Lemma A.5 and invert

$$(d_x + r) \cdot \exp\left(\frac{-t^2}{8\sigma^2}\right) \leq \delta$$

to set

$$t \approx \sqrt{T}\sigma_{\text{avg}}(1+C)\sqrt{\frac{d_x + \log(T/\delta)}{N_2} \log\left(\frac{d_x}{\delta}\right)}, \quad \text{recalling } r \leq d_x.$$

The resulting Hoeffding bound yields

$$\begin{aligned} & \mathbb{P} \left[\left\| \sum_{t=1}^T \hat{F}^{(t)\top} W_{\mathcal{N}_2}^{(t)\top} X_{\mathcal{N}_2}^{(t)} \left(\hat{\Sigma}_{x, \mathcal{N}_2}^{(t)} \right)^{-1} \right\| \geq \sqrt{T}\sigma_{\text{avg}}(1+C)\sqrt{\frac{d_x + \log(T/\delta)}{N_2} \log\left(\frac{d_x}{\delta}\right)} \right] \leq \delta \\ \iff & \mathbb{P} \left[\left\| \frac{1}{T} \sum_{t=1}^T \hat{F}^{(t)\top} W_{\mathcal{N}_2}^{(t)\top} X_{\mathcal{N}_2}^{(t)} \left(\hat{\Sigma}_{x, \mathcal{N}_2}^{(t)} \right)^{-1} \right\| \geq \sigma_{\text{avg}}(1+C)\sqrt{\frac{d_x + \log(T/\delta)}{TN_2} \log\left(\frac{d_x}{\delta}\right)} \right] \leq \delta \end{aligned}$$

■

We have bounded the noise term on the DFW representation update, demonstrating critically the bound on the noise term benefits from a scaling with the number of tasks T . The task-relevant quantity σ_{avg} quantifies that the “noise level” of the problem is an *average* over the noise-levels of each task. We note that our application of Matrix Hoeffding is rather crude, and the above bound can likely be improved in terms of $\text{polylog}(1/\delta)$ factors with stronger moment bounds on the matrix-valued self-normalized martingale terms, but this is out of the scope of this paper.

Returning to the choice of C , $C \approx 1$ implies no further system/task-specific dependence beyond the terms in $K^{(1:T)}$; however, this may translate into a stringent requirement on the burn-in N_1 and the subspace distance $\text{dist}(\hat{\Phi}, \Phi_\star)$. On the other hand, $C \gtrsim \sqrt{\kappa(\Sigma_x^{(t)})}$ relaxes the burn-in and potentially renders the subspace distance requirement trivial, but manifests a condition number in the noise bound. We note that as we expect $\text{dist}(\hat{\Phi}, \Phi_\star)$ to decrease geometrically with iterations of DFW, the subspace distance requirement is only relevant for the first few iterations. In general, this intuitively captures the cost of ill-conditioned data distributions. We now move on to bounding the contraction term.

Bounding the Contraction Term

Let us define,

$$\begin{aligned} \Delta^{(t)} &:= F_\star^{(t)} \Phi_\star \left(I_{d_x} - \hat{\Phi}^\top \hat{\Phi} \right) X_{\mathcal{N}_1}^{(t)\top} Z_{\mathcal{N}_1}^{(t)} \left(\hat{\Sigma}_{z, \mathcal{N}_1}^{(t)} \right)^{-1} \\ E^{(t)} &:= W_{\mathcal{N}_1}^{(t)\top} Z_{\mathcal{N}_1}^{(t)} \left(\hat{\Sigma}_{z, \mathcal{N}_1}^{(t)} \right)^{-1}, \end{aligned}$$

such that we may write (22) as $\hat{F}^{(t)} = F_\star^{(t)} \Phi_\star \hat{\Phi}^\top + \Delta^{(t)} + E^{(t)}$. We expand

$$\begin{aligned} \hat{F}^{(t)\top} \hat{F}^{(t)} &= \hat{\Phi} \Phi_\star^\top F_\star^{(t)\top} F_\star^{(t)} \Phi_\star \hat{\Phi}^\top + \Delta^{(t)\top} \Delta^{(t)} + E^{(t)\top} E^{(t)} \\ &\quad + \text{Sym}(\Delta^{(t)\top} F_\star^{(t)} \Phi_\star \hat{\Phi}^\top) + \text{Sym}(E^{(t)\top} F_\star^{(t)} \Phi_\star \hat{\Phi}^\top) + \text{Sym}(\Delta^{(t)\top} E^{(t)}), \end{aligned}$$

where $\text{Sym}(A) := A + A^\top$. We will make repeated use of the following matrix Cauchy-Schwarz-type lemma.

Lemma A.9 Let A_t, B_t be real-valued matrices for $t = 1, \dots, T$. Then,

$$\left\| \sum_{t=1}^T A_t B_t \right\| \leq \left\| \sum_{t=1}^T A_t A_t^\top \right\|^{1/2} \left\| \sum_{t=1}^T B_t^\top B_t \right\|^{1/2}.$$

Now taking the average over tasks T , we then may write

$$\begin{aligned} & \lambda_{\max} \left(\frac{1}{T} \sum_{t=1}^T \hat{F}^{(t)\top} \hat{F}^{(t)} \right) \\ & \leq \lambda_{\max} \left(\frac{1}{T} \sum_{t=1}^T F_\star^{(t)\top} F_\star^{(t)} \right) + \lambda_{\max} \left(\frac{1}{T} \sum_{t=1}^T \Delta^{(t)\top} \Delta^{(t)} \right) + \lambda_{\max} \left(\frac{1}{T} \sum_{t=1}^T E^{(t)\top} E^{(t)} \right) \\ & \quad + \left\| \text{Sym} \left(\frac{1}{T} \sum_{t=1}^T \Delta^{(t)\top} F_\star^{(t)} \Phi_\star \hat{\Phi}^\top \right) \right\| + \left\| \text{Sym} \left(\frac{1}{T} \sum_{t=1}^T E^{(t)\top} F_\star^{(t)} \Phi_\star \hat{\Phi}^\top \right) \right\| + \left\| \text{Sym} \left(\frac{1}{T} \sum_{t=1}^T \Delta^{(t)\top} E^{(t)} \right) \right\|. \end{aligned}$$

We observe that

$$\begin{aligned} \|\text{Sym}(A)\| &= \max_{\|u\|, \|v\|=1} u^\top A v + u^\top A^\top v \\ &\leq 2 \|A\|, \end{aligned}$$

and thus applying the above fact and Lemma A.9 on the cross terms yields

$$\begin{aligned} & \lambda_{\max} \left(\frac{1}{T} \sum_{t=1}^T \hat{F}^{(t)\top} \hat{F}^{(t)} \right) \\ & \leq \lambda_{\max} \left(\frac{1}{T} \sum_{t=1}^T F_\star^{(t)\top} F_\star^{(t)} \right) + \lambda_{\max} \left(\frac{1}{T} \sum_{t=1}^T \Delta^{(t)\top} \Delta^{(t)} \right) + \lambda_{\max} \left(\frac{1}{T} \sum_{t=1}^T E^{(t)\top} E^{(t)} \right) \\ & \quad + 2 \left\| \frac{1}{T} \sum_{t=1}^T \Delta^{(t)\top} \Delta^{(t)} \right\|^{1/2} \left\| \frac{1}{T} \sum_{t=1}^T F_\star^{(t)\top} F_\star^{(t)} \right\|^{1/2} + 2 \left\| \frac{1}{T} \sum_{t=1}^T E^{(t)\top} E^{(t)} \right\|^{1/2} \left\| \frac{1}{T} \sum_{t=1}^T F_\star^{(t)\top} F_\star^{(t)} \right\|^{1/2} \\ & \quad + 2 \left\| \frac{1}{T} \sum_{t=1}^T \Delta^{(t)\top} \Delta^{(t)} \right\|^{1/2} \left\| \frac{1}{T} \sum_{t=1}^T E^{(t)\top} E^{(t)} \right\|^{1/2}. \end{aligned}$$

Using Lemma A.6, we get the following upper bound on $\lambda_{\max} \left(\frac{1}{T} \sum_{t=1}^T \hat{F}^{(t)\top} \hat{F}^{(t)} \right)$.

Lemma A.10 Let

$$N_1 \gtrsim \max \left\{ \gamma^4 (r + \log(T/\delta)), \frac{\lambda_{\max}^{\mathbf{F}} - 1}{c_2 T} \sum_{t=1}^T \frac{\sigma_w^{(t)2} (d_y + r + \log(T/\delta))}{\lambda_{\min}(\Sigma_x^{(t)})} \right\},$$

and $\text{dist}(\hat{\Phi}, \Phi_\star) \leq \max_t \frac{4}{5} c_1 \kappa \left(\Sigma_x^{(t)} \right)^{-1}$ for given constants $c_1, c_2 \in (0, 1)$. Then, with probability at least $1 - \delta$, we have

$$\lambda_{\max} \left(\frac{1}{T} \sum_{t=1}^T \hat{F}^{(t)\top} \hat{F}^{(t)} \right) \leq (1 + 2c_1 + 2c_2 + (c_1 + c_2)^2) \lambda_{\max}^{\mathbf{F}}.$$

Proof: we see that it suffices to establish $\left\| \frac{1}{T} \sum_{t=1}^T \Delta^{(t)\top} \Delta^{(t)} \right\| \lesssim \left\| \frac{1}{T} \sum_{t=1}^T F_\star^{(t)\top} F_\star^{(t)} \right\| =: \lambda_{\max}^{\mathbf{F}}$ and $\left\| \frac{1}{T} \sum_{t=1}^T E^{(t)\top} E^{(t)} \right\| \lesssim \lambda_{\max}^{\mathbf{F}}$ in order to establish

$$\lambda_{\max} \left(\frac{1}{T} \sum_{t=1}^T \hat{F}^{(t)\top} \hat{F}^{(t)} \right) \lesssim \lambda_{\max}^{\mathbf{F}}.$$

We recall that

$$\begin{aligned} \Delta^{(t)} &:= F_\star^{(t)} \Phi_\star \left(I_{d_x} - \hat{\Phi}^\top \hat{\Phi} \right) X_{\mathcal{N}_1}^{(t)\top} Z_{\mathcal{N}_1}^{(t)} \left(\hat{\Sigma}_{z, \mathcal{N}_1}^{(t)} \right)^{-1} \\ E^{(t)} &:= W_{\mathcal{N}_1}^{(t)\top} Z_{\mathcal{N}_1}^{(t)} \left(\hat{\Sigma}_{z, \mathcal{N}_1}^{(t)} \right)^{-1}, \end{aligned}$$

which by Lemma A.6 admit the following high-probability bounds: let $|\mathcal{N}_1| := N_1 \gtrsim \gamma^4 (r + \log(T/\delta))$. Then, with probability greater than $1 - \delta$, we have for each $t \in [T]$

$$\begin{aligned} \left\| \Phi_\star \mathcal{P}_{\hat{\Phi}}^\perp X_{\mathcal{N}_1}^{(t)\top} Z_{\mathcal{N}_1}^{(t)} \left(\hat{\Sigma}_{z, \mathcal{N}_1}^{(t)} \right)^{-1} \right\| &\leq \frac{5}{4} \text{dist}(\hat{\Phi}, \Phi_\star) \kappa(\Sigma_x^{(t)}) \\ \left\| W_{\mathcal{N}_1}^{(t)\top} Z_{\mathcal{N}_1}^{(t)} \left(\hat{\Sigma}_{z, \mathcal{N}_1}^{(t)} \right)^{-1} \right\| &\lesssim \sigma_w^{(t)} \sqrt{\frac{d_y + r + \log(T/\delta)}{\lambda_{\min}(\Sigma_x^{(t)}) N_1}}. \end{aligned}$$

In particular, this implies

$$\begin{aligned} \frac{1}{T} \sum_{t=1}^T \Delta^{(t)\top} \Delta^{(t)} &\preceq \left(\frac{1}{T} \sum_{t=1}^T F_\star^{(t)} F_\star^{(t)} \right) \cdot \max_t \left(\frac{5}{4} \text{dist}(\hat{\Phi}, \Phi_\star) \kappa(\Sigma_x^{(t)}) \right)^2 \\ \left\| \frac{1}{T} E^{(t)\top} E^{(t)} \right\| &\leq \left(\frac{1}{T} \sum_{t=1}^T \frac{\sigma_w^{(t)2}}{\lambda_{\min}(\Sigma_x^{(t)})} \right) \frac{d_y + r + \log(T/\delta)}{N_1} \end{aligned}$$

It therefore suffices to set bounds on $\text{dist}(\hat{\Phi}, \Phi_\star)$ and N_1 such that $\max_t \frac{5}{4} \text{dist}(\hat{\Phi}, \Phi_\star) \kappa(\Sigma_x^{(t)}) \leq c_1$ and $\left\| \frac{1}{T} E^{(t)\top} E^{(t)} \right\| \leq c_2^2 \left\| \frac{1}{T} \sum_{t=1}^T F_\star^{(t)\top} F_\star^{(t)} \right\|$ for appropriate numerical constants c_1, c_2 . Given

$$\begin{aligned} \text{dist}(\hat{\Phi}, \Phi_\star) &\leq \max_t \frac{4}{5} c_1 \kappa(\Sigma_x^{(t)})^{-1} \\ N_1 &\gtrsim \max \left\{ \gamma^4 (r + \log(T/\delta)), \frac{\lambda_{\max}^{\mathbf{F}} - 1}{c_2^2 T} \sum_{t=1}^T \frac{\sigma_w^{(t)2} (d_y + r + \log(T/\delta))}{\lambda_{\min}(\Sigma_x^{(t)})} \right\}, \end{aligned}$$

we have

$$\lambda_{\max} \left(\frac{1}{T} \sum_{t=1}^T \hat{F}^{(t)\top} \hat{F}^{(t)} \right) \leq (1 + 2c_1 + 2c_2 + (c_1 + c_2)^2) \lambda_{\max} \left(\frac{1}{T} \sum_{t=1}^T F_\star^{(t)\top} F_\star^{(t)} \right)$$

■

Lemma A.10 informs the maximum we may set the step-size. To now upper bound the contraction rate, we lower bound $\lambda_{\min}(\hat{F}^{(t)\top} \hat{F}^{(t)})$. We observe that the diagonal terms $\Delta^{(t)\top} \Delta^{(t)}, E^{(t)\top} E^{(t)}$ are

psd, and thus can be ignored in the lower bound. We then observe that by Weyl's inequality [Horn and Johnson, 2012], we have

$$\lambda_{\min}\left(\frac{1}{T}\sum_{t=1}^T\hat{F}^{(t)\top}\hat{F}^{(t)}\right)\geq\lambda_{\min}\left(\frac{1}{T}\sum_{t=1}^T\hat{\Phi}\Phi_{\star}^{\top}F_{\star}^{(t)\top}F_{\star}^{(t)}\Phi_{\star}\hat{\Phi}^{\top}\right) - \lambda_{\max}\left(\frac{1}{T}\sum_{t=1}^T\text{Sym}(\Delta^{(t)\top}F_{\star}^{(t)}\Phi_{\star}\hat{\Phi}^{\top})+\text{Sym}(E^{(t)\top}F_{\star}^{(t)}\Phi_{\star}\hat{\Phi}^{\top})+\text{Sym}(\Delta^{(t)\top}E^{(t)})\right).$$

Just as in the upper bound of $\lambda_{\max}(\frac{1}{T}\sum_{t=1}^T\hat{F}^{(t)\top}\hat{F}^{(t)})$, it suffices to upper bound the cross terms. Therefore, following the same proof as Lemma A.10, we have the analogous result.

Lemma A.11 *Let*

$$N_1\gtrsim\max\left\{\gamma^4(r+\log(T/\delta)),\frac{\lambda_{\min}^{\mathbf{F}}-1}{b_2^2}\frac{1}{T}\sum_{t=1}^T\frac{\sigma_w^{(t)2}(d_y+r+\log(T/\delta))}{\lambda_{\min}(\Sigma_x^{(t)})}\right\},$$

and $\text{dist}(\hat{\Phi},\Phi_{\star})\leq\frac{4}{5}b_1\sqrt{\frac{\lambda_{\min}^{\mathbf{F}}}{\lambda_{\max}^{\mathbf{F}}}}\max_t\kappa(\Sigma_x^{(t)})^{-1}$ for given constants $b_1, b_2 \in (0, 1)$. Then, with probability at least $1 - \delta$, we have

$$\lambda_{\min}\left(\frac{1}{T}\sum_{t=1}^T\hat{F}^{(t)\top}\hat{F}^{(t)}\right)\geq\left(\left(1-\frac{2}{3}b_1^2\right)-2(b_1+b_2+b_1b_2)\right)\lambda_{\min}^{\mathbf{F}}.$$

Proof: as in Lemma A.10, we invert the bounds from Lemma A.6 for our desired factors of $\lambda_{\min}^{\mathbf{F}}$. In particular, observing

$$\begin{aligned}\left\|\Phi_{\star}\mathcal{P}_{\hat{\Phi}}^{\perp}X_{\mathcal{N}_1}^{(t)\top}Z_{\mathcal{N}_1}^{(t)}\left(\hat{\Sigma}_{z,\mathcal{N}_1}^{(t)}\right)^{-1}\right\|&\leq\frac{5}{4}\text{dist}(\hat{\Phi},\Phi_{\star})\kappa(\Sigma_x^{(t)}) \\ \left\|\frac{1}{T}\sum_{t=1}^TW_{\mathcal{N}_1}^{(t)\top}Z_{\mathcal{N}_1}^{(t)}\left(\hat{\Sigma}_{z,\mathcal{N}_1}^{(t)}\right)^{-1}\right\|&\lesssim\frac{1}{T}\sum_{t=1}^T\sigma_w^{(t)}\sqrt{\frac{d_y+r+\log(1/\delta)}{\lambda_{\min}(\Sigma_x^{(t)})N_1}},\end{aligned}$$

we invert the RHS' for $b_1\sqrt{\frac{\lambda_{\min}^{\mathbf{F}}}{\lambda_{\max}^{\mathbf{F}}}}$ and $b_2\sqrt{\lambda_{\min}^{\mathbf{F}}}$, respectively, to yield our proposed burn-in and the following guarantee with probability at least $1 - \delta$

$$\begin{aligned}&\lambda_{\max}\left(\text{Sym}(\Delta^{(t)\top}F_{\star}^{(t)}\Phi_{\star}\hat{\Phi}^{\top})+\text{Sym}(E^{(t)\top}F_{\star}^{(t)}\Phi_{\star}\hat{\Phi}^{\top})+\text{Sym}(\Delta^{(t)\top}E^{(t)})\right) \\ &\leq 2(b_1+b_2+b_1b_2)\lambda_{\min}^{\mathbf{F}}.\end{aligned}$$

The only additional factor we account for here is the lower bound on $\lambda_{\min}\left(\frac{1}{T}\sum_{t=1}^T\hat{\Phi}\Phi_{\star}^{\top}F_{\star}^{(t)\top}F_{\star}^{(t)}\Phi_{\star}\hat{\Phi}^{\top}\right)$. We have

$$\begin{aligned}\lambda_{\min}\left(\frac{1}{T}\sum_{t=1}^T\hat{\Phi}\Phi_{\star}^{\top}F_{\star}^{(t)\top}F_{\star}^{(t)}\Phi_{\star}\hat{\Phi}^{\top}\right) &= \min_{\|x\|=1}x^{\top}\hat{\Phi}\Phi_{\star}^{\top}\left(\frac{1}{T}\sum_{t=1}^TF_{\star}^{(t)\top}F_{\star}^{(t)}\right)\Phi_{\star}\hat{\Phi}^{\top}x \\ &\geq\lambda_{\min}\left(\frac{1}{T}\sum_{t=1}^TF_{\star}^{(t)\top}F_{\star}^{(t)}\right)\min_{\|x\|=1}x^{\top}\hat{\Phi}\Phi_{\star}^{\top}\Phi_{\star}\hat{\Phi}^{\top}x \\ &=\lambda_{\min}\left(\frac{1}{T}\sum_{t=1}^TF_{\star}^{(t)\top}F_{\star}^{(t)}\right)\sigma_{\min}^2\left(\Phi_{\star}\hat{\Phi}^{\top}\right).\end{aligned}$$

To further lower bound $\sigma_{\min}^2(\Phi_\star \hat{\Phi}^\top)$, we observe that

$$\begin{aligned} \hat{\Phi} \hat{\Phi}^\top &= \hat{\Phi} \left(\Phi_\star^\top \Phi_\star + \Phi_{\star,\perp}^\top \Phi_{\star,\perp} \right) \hat{\Phi}^\top \\ \implies 1 = \lambda_{\max}(\hat{\Phi} \hat{\Phi}^\top) &\leq \lambda_{\min} \left(\hat{\Phi} \Phi_\star^\top \Phi_\star \hat{\Phi}^\top \right) + \lambda_{\max} \left(\hat{\Phi} \Phi_{\star,\perp}^\top \Phi_{\star,\perp} \hat{\Phi}^\top \right) \quad \text{Weyl's inequality} \\ \implies \sigma_{\min}^2(\Phi_\star \hat{\Phi}^\top) &\geq 1 - \left\| \Phi_{\star,\perp} \hat{\Phi}^\top \right\|^2 =: 1 - \text{dist}(\hat{\Phi}, \Phi_\star)^2. \end{aligned}$$

Under our assumption ensuring $\text{dist}(\hat{\Phi}, \Phi_\star) \leq \frac{4}{5} b_1 \sqrt{\frac{\lambda_{\min}^{\mathbf{F}}}{\lambda_{\max}^{\mathbf{F}}}} \max_t \kappa(\Sigma_x^{(t)})^{-1} \leq \frac{4}{5} b_1$, we can piece together this bound with the bound on the cross terms to yield with probability at least $1 - \delta$

$$\lambda_{\min} \left(\frac{1}{T} \sum_{t=1}^T \hat{F}^{(t)\top} \hat{F}^{(t)} \right) \geq \left(\left(1 - \frac{2}{3} b_1^2\right) - 2(b_1 + b_2 + b_1 b_2) \right) \lambda_{\min} \left(\frac{1}{T} \sum_{t=1}^T F_\star^{(t)\top} F_\star^{(t)} \right),$$

which completes the proof. \blacksquare

Piecing together Lemma A.10 and Lemma A.11, and observing that if $b_1 = c_1$, $b_2 = c_2$, the burn-in of Lemma A.11 dominates Lemma A.10, we get the following bound on the contraction factor

Lemma A.12 *Let*

$$N_1 \gtrsim \max \left\{ \gamma^4 (r + \log(T/\delta)), \frac{\lambda_{\min}^{\mathbf{F}} - 1}{b_2^2} \frac{1}{T} \sum_{t=1}^T \frac{\sigma_w^{(t)2} (d_y + r + \log(T/\delta))}{\lambda_{\min}(\Sigma_x^{(t)})} \right\},$$

and $\text{dist}(\hat{\Phi}, \Phi_\star) \leq \frac{4}{5} b_1 \sqrt{\frac{\lambda_{\min}^{\mathbf{F}}}{\lambda_{\max}^{\mathbf{F}}}} \max_t \kappa(\Sigma_x^{(t)})^{-1}$ for given constants $b_1, b_2 \in (0, 1)$. Then, for step-size satisfying $\eta \leq \frac{1}{(1+2b_1+2b_2+(b_1+b_2)^2)\lambda_{\max}^{\mathbf{F}}}$, with probability at least $1 - \delta$, we have

$$\left\| I_{d_x} - \eta \frac{1}{T} \sum_{t=1}^T \hat{F}^{(t)\top} \hat{F}^{(t)} \right\| \leq \left(1 - \left(\left(1 - \frac{2}{3} b_1^2\right) - 2(b_1 + b_2 + b_1 b_2) \right) \eta \lambda_{\min}^{\mathbf{F}} \right).$$

We make a couple of qualitative remarks here:

- When b_1, b_2 are small, and η is set to its maximal permitted value, then the contraction rate approaches $\left(1 - \frac{\lambda_{\min}^{\mathbf{F}}}{\lambda_{\max}^{\mathbf{F}}}\right)$, which is intuitively the best one can hope for by inspecting the contraction factor $I - \frac{\eta}{T} \sum_{t=1}^T \hat{F}^{(t)\top} \hat{F}^{(t)}$.
- Though the above initialization requirement on $\text{dist}(\hat{\Phi}, \Phi_\star)$ may be relevant during the early iterations, we note that due to the exponential convergence ensured by Lemma A.12, the requirement (i.e. b_1) can be scaled down exponentially quickly, leaving the dominant barrier the burn-in requirement on N_1 .

The last remaining step is to bound the effect of the orthogonalization factor R . We want to upper bound $\|R^{-1}\| = 1/\sigma_{\min}(R)$, and thus it suffices to lower bound $\sigma_{\min}(R)$. By definition, we

have

$$\begin{aligned}
RR^\top &= (R\hat{\Phi}_+)(R\hat{\Phi}_+)^\top \\
&= \left(\hat{\Phi} - \frac{\eta}{T} \sum_{t=1}^T \hat{F}^{(t)\top} \left(\hat{F}^{(t)} \hat{\Phi} - F_\star^{(t)} \Phi_\star \right) - \frac{\eta}{T} \sum_{t=1}^T \hat{F}^{(t)\top} W^{(t)\top} X^{(t)} \left(\hat{\Sigma}_x^{(t)} \right)^{-1} \right) \\
&\quad \left(\hat{\Phi} - \frac{\eta}{T} \sum_{t=1}^T \hat{F}^{(t)\top} \left(\hat{F}^{(t)} \hat{\Phi} - F_\star^{(t)} \Phi_\star \right) - \frac{\eta}{T} \sum_{t=1}^T \hat{F}^{(t)\top} W^{(t)\top} X^{(t)} \left(\hat{\Sigma}_x^{(t)} \right)^{-1} \right)^\top \\
&\succeq I_r - \underbrace{\text{Sym} \left(\frac{\eta}{T} \sum_{t=1}^T \hat{F}^{(t)\top} \left(\hat{F}^{(t)} \hat{\Phi} - F_\star^{(t)} \Phi_\star \right) \hat{\Phi}^\top \right)}_{(a)} - \underbrace{\text{Sym} \left(\frac{\eta}{T} \sum_{t=1}^T \hat{F}^{(t)\top} W^{(t)\top} X^{(t)} \left(\hat{\Sigma}_x^{(t)} \right)^{-1} \hat{\Phi}^\top \right)}_{(b)} \\
&\quad + \underbrace{\text{Sym} \left(\frac{\eta^2}{T^2} \hat{F}^{(t)\top} \left(\hat{F}^{(t)} \hat{\Phi} - F_\star^{(t)} \Phi_\star \right)^\top \left(\sum_{t=1}^T \hat{F}^{(t)\top} W^{(t)\top} X^{(t)} \left(\hat{\Sigma}_x^{(t)} \right)^{-1} \right)^\top \right)}_{(c)},
\end{aligned}$$

where, besides $\hat{\Phi} \hat{\Phi}^\top = I_r$, we have discarded the pd diagonal terms of the expansion. Intuitively, we will show that under appropriate burn-in conditions $\left\| \frac{1}{T} \sum_{t=1}^T \hat{F}^{(t)\top} \left(\hat{F}^{(t)} \hat{\Phi} - F_\star^{(t)} \Phi_\star \right) \right\| \lesssim \lambda_{\min}^{\mathbf{F}}$ and $\left\| \frac{1}{T} \sum_{t=1}^T \hat{F}^{(t)\top} W^{(t)\top} X^{(t)} \left(\hat{\Sigma}_x^{(t)} \right)^{-1} \right\| \lesssim \lambda_{\min}^{\mathbf{F}}$, which will in turn imply

$$RR^\top \succcurlyeq (1 - c\eta\lambda_{\min}^{\mathbf{F}})I_r \implies 1/\sigma_{\min}(R) \lesssim (1 - c\eta\lambda_{\min}^{\mathbf{F}})^{-1/2},$$

which deflates the effective contraction rate established in Lemma A.12 by a square-root. It remains to establish the requisite bounds on the cross-terms.

Focusing on the first cross term (a), we have

$$\begin{aligned}
&\text{Sym} \left(\frac{\eta}{T} \sum_{t=1}^T \hat{F}^{(t)\top} \left(\hat{F}^{(t)} \hat{\Phi} - F_\star^{(t)} \Phi_\star \right) \hat{\Phi}^\top \right) \\
&= \frac{\eta}{T} \sum_{t=1}^T \text{Sym} \left(\hat{F}^{(t)\top} \left(\hat{F}^{(t)} - F_\star^{(t)} \Phi_\star \hat{\Phi}^\top \right) \right) \\
&= \frac{\eta}{T} \sum_{t=1}^T \text{Sym} \left(\hat{F}^{(t)\top} \left(\Delta^{(t)} + E^{(t)} \right) \right) \\
&= \frac{\eta}{T} \sum_{t=1}^T \text{Sym} \left(\left(F_\star^{(t)} \Phi_\star \hat{\Phi}^\top + \Delta^{(t)} + E^{(t)} \right)^\top \left(\Delta^{(t)} + E^{(t)} \right) \right) \\
&= \frac{\eta}{T} \sum_{t=1}^T \text{Sym} \left(\hat{\Phi} \Phi_\star^\top F_\star^{(t)\top} \Delta^{(t)} + \hat{\Phi} \Phi_\star^\top F_\star^{(t)\top} E^{(t)} \right) + 2\Delta^{(t)\top} \Delta^{(t)} + 2E^{(t)\top} E^{(t)} + 2\text{Sym} \left(\Delta^{(t)\top} E^{(t)} \right).
\end{aligned}$$

Much like for Lemma A.11, it suffices to determine bounds on $\text{dist}(\hat{\Phi}, \Phi_\star)$ and N_1 such that the individual terms above are upper bounded by a desired constant factor of $\lambda_{\min}^{\mathbf{F}}$. For given

$c_1, c_2 \in (0, 1)$, if the following hold:

$$\begin{aligned} \text{dist}(\hat{\Phi}, \Phi_*) &\leq c_1 \sqrt{\frac{\lambda_{\min}^{\mathbf{F}}}{\lambda_{\max}^{\mathbf{F}}}} \max_t \kappa(\Sigma_x^{(t)})^{-1} \\ N_1 &\gtrsim \frac{\lambda_{\min}^{\mathbf{F}}}{c_2^2} \frac{1}{T} \sum_{t=1}^T \frac{\sigma_w^{(t)2} (d_y + r + \log(1/\delta))}{\lambda_{\min}(\Sigma_x^{(t)})}, \end{aligned}$$

then we have

$$\lambda_{\max} \left(\text{Sym} \left(\frac{\eta}{T} \sum_{t=1}^T \hat{F}^{(t)\top} \left(\hat{F}^{(t)} \hat{\Phi} - F_{\star}^{(t)} \Phi_* \right) \hat{\Phi}^{\top} \right) \right) \leq 2 \left(c_1 + c_2 + 2(c_1 + c_2)^2 \right) \eta \lambda_{\min}^{\mathbf{F}}.$$

Now we notice the second cross term (b) is precisely the noise term considered in Appendix A.2, and thus given the burn-in

$$\begin{aligned} N_1 &\gtrsim \max \left\{ \gamma^4 (r + \log(T/\delta)), \max_t \frac{\sigma_w^{(t)2}}{C^2 \|F_{\star}^{(t)}\|^2 \lambda_{\min}(\Sigma_x^{(t)})} (d_y + r + \log(T/\delta)) \right\}, \\ N_2 &\gtrsim \gamma^4 (d_x + \log(T/\delta)), \end{aligned}$$

and $\text{dist}(\hat{\Phi}, \Phi_*) \leq \max_t \frac{2}{5} C \kappa(\Sigma_x^{(t)})^{-1}$, for fixed $C > 0$, with probability at least $1 - \delta$,

$$\left\| \frac{1}{T} \sum_{t=1}^T \hat{F}^{(t)\top} W_{\mathcal{N}_2}^{(t)\top} X_{\mathcal{N}_2}^{(t)} \left(\hat{\Sigma}_{x, \mathcal{N}_2}^{(t)} \right)^{-1} \right\| \lesssim \sigma_{\text{avg}} (1 + C) \sqrt{\frac{d_x + \log(T/\delta)}{TN_2} \log\left(\frac{d_x}{\delta}\right)},$$

where we recall $\sigma_{\text{avg}} := \sqrt{\frac{1}{T} \sum_{t=1}^T \frac{\sigma_w^{(t)2} \|F_{\star}^{(t)}\|^2}{\lambda_{\min}(\Sigma_x^{(t)})}}$ is the *task-averaged* noise-level. Setting $C = 2b_1$ (where $b_1 \leq 1/2$ is determined in Lemma A.11), the requirement on $\text{dist}(\hat{\Phi}, \Phi_*)$ becomes redundant and $(1 + C) \leq 2$. Then, we may invert the RHS of the above inequality for $c_3 \lambda_{\min}^{\mathbf{F}}$ to yield a burn-in on TN_2 : setting

$$TN_2 \gtrsim \frac{\lambda_{\min}^{\mathbf{F}}}{c_3^2} \sigma_{\text{avg}}^2 (d_x + \log(T/\delta)) \log\left(\frac{d_x}{\delta}\right),$$

then with probability at least $1 - \delta$

$$\lambda_{\max} \left(\text{Sym} \left(\frac{\eta}{T} \sum_{t=1}^T \hat{F}^{(t)\top} W^{(t)\top} X^{(t)} \left(\hat{\Sigma}_x^{(t)} \right)^{-1} \hat{\Phi}^{\top} \right) \right) \leq c_3 \eta \lambda_{\min}^{\mathbf{F}}.$$

We note that the third and last cross term (c) is bounded by the product of our bounds on the first two cross terms, which under our conditions are both bounded by 1. Piecing these bounds together yields the following bound on the orthogonalization factor.

Lemma A.13 *Let the following burn-in conditions hold:*

$$\begin{aligned} \text{dist}(\hat{\Phi}, \Phi_\star) &\leq \frac{4}{5} c_1 \sqrt{\frac{\lambda_{\min}^{\mathbf{F}}}{\lambda_{\max}^{\mathbf{F}}}} \max_t \kappa(\Sigma_x^{(t)})^{-1} \\ N_1 &\gtrsim \max \left\{ \gamma^4 (r + \log(T/\delta)), \max_t \frac{\sigma_w^{(t)2}}{c_1^2 \|F_\star^{(t)}\|^2 \lambda_{\min}(\Sigma_x^{(t)})} (d_y + r + \log(T/\delta)), \right. \\ &\quad \left. \frac{\lambda_{\min}^{\mathbf{F}}}{c_2^2} \frac{1}{T} \sum_{t=1}^T \frac{\sigma_w^{(t)2}}{\lambda_{\min}(\Sigma_x^{(t)})} (d_y + r + \log(T/\delta)) \right\}, \\ N_2 &\gtrsim \max \left\{ \gamma^4 (d_x + \log(T/\delta)), \frac{\lambda_{\min}^{\mathbf{F}}}{c_3^2} \frac{\sigma_{\text{avg}}^2}{T} (d_x + \log(T/\delta)) \log\left(\frac{d_x}{\delta}\right) \right\}, \end{aligned}$$

where $c_1, c_2, c_3 \in (0, 1/2)$ are fixed constants. Then, given $\eta \leq \frac{1}{(1+2c_1+2c_2+(c_1+c_2)^2)\lambda_{\max}^{\mathbf{F}}}$, with probability at least $1 - \delta$, we have the following bound on the orthogonalization factor R :

$$\|R^{-1}\| \leq (1 - (c + c_3 + c \cdot c_3) \eta \lambda_{\min}^{\mathbf{F}})^{-1/2},$$

where $c := 2(c_1 + c_2 + 2(c_1 + c_2)^2)$.

We are now ready to combine Lemma A.12 and Lemma A.13 to yield the full high-probability descent guarantee for DFW. From those lemmas, we have the free parameters b_1, b_2 and c_1, c_2, c_3 that trade-off between the burn-in and the contraction factor. Recall the upper bound on our contraction factor scales as

$$\begin{aligned} &\|R^{-1}\| \cdot \left\| I_{d_x} - \eta \frac{1}{T} \sum_{t=1}^T \hat{F}^{(t)\top} \hat{F}^{(t)} \right\| \\ &\leq \frac{1 - \left((1 - \frac{2}{3} b_1^2) - 2(b_1 + b_2 + b_1 b_2) \right) \eta \lambda_{\min}^{\mathbf{F}}}{\sqrt{1 - (c + c_3 + c \cdot c_3) \eta \lambda_{\min}^{\mathbf{F}}}}. \end{aligned} \tag{28}$$

To simplify the above, it suffices to set $b_1 = c_1, b_2 = c_2$. Therefore, for sufficiently small c_1, c_2, c_3 , the factor preceding $\eta \lambda_{\min}^{\mathbf{F}}$ in the numerator will be larger than that on the denominator, which allows us to upper bound the whole contraction factor as simply the square-root of the numerator, as in Collins et al. [2021]. However, slowing the contraction rate by a square root is qualitatively wasteful, as for sufficiently small c_1, c_2 , the numerator approaches $1 - \eta \lambda_{\min}^{\mathbf{F}}$, while the denominator approaches 1. Therefore, we should expect that the rate should typically not suffer the square-root, captured in the following derivation.

Lemma A.14 *Given $a_1, a_2, d \in (0, 1)$ and $\varepsilon \in (0, 1)$, if $\varepsilon \geq a_2/a_1$, then the following holds:*

$$\frac{1 - a_1 d}{\sqrt{1 - a_2 d}} < 1 - (1 - \varepsilon) a_1 d.$$

Additionally, as long as $\varepsilon \leq 1 - \frac{1 - \sqrt{1 - a_1 d}}{a_1 d}$, then $1 - (1 - \varepsilon) a_1 d \leq \sqrt{1 - a_1 d}$.

Proof of Lemma A.14: squaring the desired inequality and re-arranging some terms, we arrive at

$$\begin{aligned} a_2 &\leq \frac{1}{d} \left(1 - \frac{(1 - a_1 d)^2}{(1 - (1 - \varepsilon) a_1 d)^2} \right) \\ &= \frac{1}{d} \left(1 - \underbrace{\frac{1 - a_1 d}{1 - (1 - \varepsilon) a_1 d}}_{<1} \right) \underbrace{\left(1 + \frac{1 - a_1 d}{1 - (1 - \varepsilon) a_1 d} \right)}_{>1}. \end{aligned}$$

To certify the above inequality, it suffices to lower-bound the RHS. Since $a_1, a_2, d \in (0, 1)$, the last factor is at least 1, such that we have

$$\begin{aligned} \frac{1}{d} \left(1 - \frac{1 - a_1 d}{1 - (1 - \varepsilon) a_1 d} \right) \left(1 + \frac{1 - a_1 d}{1 - (1 - \varepsilon) a_1 d} \right) &> \frac{1}{d} \left(1 - \frac{1 - a_1 d}{1 - (1 - \varepsilon) a_1 d} \right) \\ &= \frac{1}{d} \frac{(1 - \varepsilon) a_1 d}{1 - (1 - \varepsilon) a_1 d} \\ &> \varepsilon a_1. \end{aligned}$$

Therefore, $a_2 \leq \varepsilon a_1$ is sufficient for certifying the desired inequality. The latter claim follows by squaring and rearranging terms to yield the quadratic inequality:

$$(1 - \varepsilon)^2 a_1 d - 2(1 - \varepsilon) + 1 \leq 0,$$

Setting $\lambda := 1 - \varepsilon$, the solution interval is $\lambda \in \left(\frac{1 - \sqrt{1 - a_1 d}}{a_1 d}, \frac{1 + \sqrt{1 - a_1 d}}{a_1 d} \right)$. The upper limit is redundant as it exceeds 1 and $\varepsilon \in (0, 1)$, leaving the lower limit as the condition on ε proposed in the lemma. \blacksquare

To operationalize Lemma A.14, taking $d := \eta \lambda_{\min}^{\mathbf{F}}$, a_1 as the constants on the numerator of (28), and a_2 as the constants on the denominator, as long as we choose c_1, c_2, c_3 such that a_2 is smaller than a given fraction of a_1 , then the descent rate is essentially preserved after accounting for the orthonormalization factor. The latter claim captures that avoiding the square-root is “worth it” as long as $a_1 d$ is not too close to 1, which is usually satisfied considering $d = \eta \lambda_{\min}^{\mathbf{F}}$ is at largest $\frac{1}{(1 + 2c_1 + 2c_2 + (c_1 + c_2)^2)} \frac{\lambda_{\min}^{\mathbf{F}}}{\lambda_{\max}^{\mathbf{F}}}$ by Lemma A.13. Therefore, choosing $a_3 := (1 + 2c_1 + 2c_2 + (c_1 + c_2)^2)$, we can ensure our choice of ε is valid independent of $\lambda_{\min}^{\mathbf{F}}, \lambda_{\max}^{\mathbf{F}}$ by checking $\varepsilon \leq 1 - \frac{1 - \sqrt{1 - a_1/a_3}}{a_1/a_3}$. Since this implies the choice of ε must satisfy a lower and upper bound $\varepsilon \in \left(\frac{a_2}{a_1}, 1 - \frac{1 - \sqrt{1 - a_1/a_3}}{a_1/a_3} \right)$ in terms of a function of our universal constants in a_1, a_2, a_3 in order to fulfill the improved convergence rate, we must do our due diligence and instantiate choices of universal constants c_1, c_2, c_3 to certify that this acceleration holds universally, independent of problem-dependent parameters.

We note that c_1, c_2 also controls the upper bound on η in Lemma A.13, with smaller c_1, c_2 leading to an upper bound approaching $\eta \leq 1/\lambda_{\max}^{\mathbf{F}}$. For the purposes of this work, it suffices to set $c_1 \leftarrow 1/80, c_2 = c_3 \leftarrow 1/100$. Conditioned on the events of Proposition A.2, Lemma A.12,

Lemma A.13, then plugging in these constants yield the following:

$$\begin{aligned}
a_1 &= \left(1 - \frac{2}{3}c_1^2\right) - 2(c_1 + c_2 + c_1c_2) \approx 0.955 \\
a_2 &= c + c_3 + c \cdot c_3 \approx 0.0575 \\
a_3 &= 1 + 2c_1 + 2c_2 + (c_1 + c_2)^2 \approx 1.046 \\
\varepsilon &\in \left[\frac{a_2}{a_1}, 1 - \frac{1 - \sqrt{1 - a_1/a_3}}{a_1/a_3}\right] \approx [0.0602, 0.228] \neq \emptyset \\
\Rightarrow \left\| R^{-1} \cdot \left\| I_{d_x} - \eta \frac{1}{T} \sum_{t=1}^T \hat{F}^{(t)\top} \hat{F}^{(t)} \right\| \right\| &\leq (1 - (1 - \varepsilon)a_1\eta\lambda_{\min}^{\mathbf{F}}) \\
&\leq 1 - 0.897\eta\lambda_{\min}^{\mathbf{F}} \quad \text{setting } \varepsilon = a_2/a_1 \\
\eta &\leq \frac{1}{a_3} \frac{1}{\lambda_{\max}^{\mathbf{F}}} \approx 0.956 \frac{1}{\lambda_{\max}^{\mathbf{F}}}.
\end{aligned}$$

Theorem A.1 (Full version of Theorem 3.1, iid) *Let Assumption 3.1 hold. Let the following burn-in conditions hold:*

$$\begin{aligned}
\text{dist}(\hat{\Phi}, \Phi_*) &\leq \frac{1}{100} \sqrt{\frac{\lambda_{\min}^{\mathbf{F}}}{\lambda_{\max}^{\mathbf{F}}}} \max_t \kappa(\Sigma_x^{(t)})^{-1} \\
N_1 &\gtrsim \max \left\{ \gamma^4 (r + \log(T/\delta)), \bar{\sigma}_{\mathbf{F}}^2 (d_y + r + \log(T/\delta)) \right\}, \\
N_2 &\gtrsim \max \left\{ \gamma^4 (d_x + \log(T/\delta)), \lambda_{\min}^{\mathbf{F}}^{-1} \frac{\sigma_{\text{avg}}^2}{T} (d_x + \log(T/\delta)) \log\left(\frac{d_x}{\delta}\right) \right\},
\end{aligned}$$

where $\bar{\sigma}_{\mathbf{F}}^2 := \max \left\{ \max_t \frac{\sigma_w^{(t)2}}{\|F_*^{(t)}\|^2 \lambda_{\min}(\Sigma_x^{(t)})}, \frac{1}{T} \sum_{t=1}^T \frac{\sigma_w^{(t)2}}{\lambda_{\min} \lambda_{\min}(\Sigma_x^{(t)})} \right\}$. Then, given step-size satisfying $\eta \leq 0.956 \lambda_{\max}^{\mathbf{F}}^{-1}$, running an iteration of DFW yields an updated representation $\hat{\Phi}_+$ that satisfies with probability at least $1 - \delta$:

$$\text{dist}(\hat{\Phi}_+, \Phi_*) \leq (1 - 0.897\eta\lambda_{\min}^{\mathbf{F}}) \text{dist}(\hat{\Phi}, \Phi_*) + C \cdot \sigma_{\text{avg}} \sqrt{\frac{d_x + \log(T/\delta)}{TN_2} \log\left(\frac{d_x}{\delta}\right)},$$

where $C > 0$ is a universal constant and $\sigma_{\text{avg}} := \sqrt{\frac{1}{T} \sum_{t=1}^T \frac{\sigma_w^{(t)2} \|F_*^{(t)}\|^2}{\lambda_{\min}(\Sigma_x^{(t)})}}$ is the task-averaged noise level.

A.3 The Non-IID Setting

To extend our analysis to the non-iid setting, we first instantiate our covariates as β -mixing stationary processes [Kuznetsov and Mohri, 2017, Yu, 1994], recalling Assumption 3.1:

Assumption A.1 (Geometric mixing) *For each $t \in [T]$, assume the process $\{x_i^{(t)}\}_{t \geq 1}$ is a mean-zero stationary β -mixing process, with stationary covariance $\Sigma_x^{(t)}$ and $\beta^{(t)}(k) := \Gamma^{(t)} \mu^{(t)k}$.*

We note that exact stationarity is unnecessary as long as the marginal distributions converge to stationarity sufficiently fast; however, we assume exact stationarity for notational convenience. We now invoke the blocking technique on each trajectory, where each trajectory is subsampled into a

trajectories of length m (where we assume a divides N for notational convenience), by assigning each a -th point to a trajectory. We may then apply the analysis of the iid setting on a deflated dataset of $T \cdot m$ data points *drawn from the respective stationary distributions*. Now applying Lemma A.4, setting $g(\cdot)$ as the indicator function for the burn-in requirements of and the final descent bound of Theorem A.1, we have for all $j = 1, \dots, a$.

$$\left| \mathbb{E} \left[g \left(\left\{ X_{\infty}^{(t), Nm} \right\}_{t \in [T]} \right) \right] - \mathbb{E} \left[g \left\{ X_{(j)}^{(t), NT} \right\}_{t \in [T]} \right] \right| \leq m\beta(a) \leq \delta'$$

Setting $\delta' = \delta/a$ and union bounding over each $j = 1, \dots, a$, we may invert $N\beta(a) = \delta$ to find $a = \tau_{\text{mix}}^{(t)} := \left(\frac{\log(\Gamma^{(t)}N/\delta)}{\log(1/\mu^{(t)})} \vee 1 \right)$. This yields the final descent guarantee adjusting for mixing:

Theorem A.2 (Full version of Theorem 3.1, mixing) *Let Assumption 3.1 hold. Let the following burn-in conditions hold:*

$$\begin{aligned} \text{dist}(\hat{\Phi}, \Phi_{\star}) &\leq \frac{1}{100} \sqrt{\frac{\lambda_{\min}^{\mathbf{F}}}{\lambda_{\max}^{\mathbf{F}}}} \max_t \kappa \left(\Sigma_x^{(t)} \right)^{-1} \\ N_1 &\gtrsim \max_t \tau_{\text{mix}}^{(t)} \cdot \max \left\{ \gamma^4 (r + \log(T/\delta)), \bar{\sigma}_{\mathbf{F}}^2 (d_y + r + \log(T/\delta)) \right\}, \\ N_2 &\gtrsim \max_t \tau_{\text{mix}}^{(t)} \cdot \max \left\{ \gamma^4 (d_x + \log(T/\delta)), \lambda_{\min}^{\mathbf{F}}^{-1} \frac{\sigma_{\text{avg}}^2}{T} (d_x + \log(T/\delta)) \log \left(\frac{d_x}{\delta} \right) \right\}, \end{aligned}$$

where $\bar{\sigma}_{\mathbf{F}}^2 := \max \left\{ \max_t \frac{\sigma_w^{(t)2}}{\|F_{\star}^{(t)}\|^2 \lambda_{\min}(\Sigma_x^{(t)})}, \frac{1}{T} \sum_{t=1}^T \frac{\sigma_w^{(t)2}}{\lambda_{\min}^{\mathbf{F}} \lambda_{\min}(\Sigma_x^{(t)})} \right\}$. Then, given step-size satisfying $\eta \leq 0.956 \lambda_{\max}^{\mathbf{F}}^{-1}$, running an iteration of DFW yields an updated representation $\hat{\Phi}_+$ that satisfies with probability at least $1 - \delta$:

$$\text{dist}(\hat{\Phi}_+, \Phi_{\star}) \leq (1 - 0.897\eta\lambda_{\min}^{\mathbf{F}}) \text{dist}(\hat{\Phi}, \Phi_{\star}) + C \cdot \sigma_{\text{avg}} \sqrt{\frac{d_x + \log(T/\delta)}{TN_2} \log \left(\frac{d_x}{\delta} \right)},$$

where $C > 0$ is a universal constant and $\sigma_{\text{avg}} := \sqrt{\frac{1}{T} \sum_{t=1}^T \frac{\tau_{\text{mix}}^{(t)} \sigma_w^{(t)2} \|F_{\star}^{(t)}\|^2}{\lambda_{\min}(\Sigma_x^{(t)})}}$ is the task-averaged noise level.

In short, for geometric mixing processes, our algorithm guarantees hold as in the iid setting, deflated effectively by a $\log(N/\delta)$ factor. In particular, past the burn-in, the effect of mixing on the descent rate is averaged across tasks.

A.4 Converting to Sample Complexity Bounds

To highlight the importance of the task scaling T in our descent guarantees, we demonstrate how to convert general descent lemmas to sample complexity guarantees.

Lemma A.15 *For a sequence of positive integers $\{M_k\}_{k \geq 1} \subset \mathbb{N}$, define $\{d_k\}_{k \geq 1} \subset \mathbb{R}_+$ as a sequence of non-negative real numbers dependent on $\{M_k\}$ that satisfy the relation*

$$d_{k+1} \leq \rho \cdot d_k + \frac{C}{M_k},$$

for some $\rho \in (0, 1)$ and $C > 0$. Let $d_0 = \tau$. Given a positive integer M , we may partition $M = \sum_{k=1}^K M_k$, where

$$K := \left\lceil \frac{1}{2} \log \left(\frac{2}{1+\rho} \right)^{-1} \frac{M\tau^2}{C} \left(\frac{1-\rho}{2} \right)^3 + 1 \right\rceil,$$

such that the following guarantee holds on d_K :

$$d_K \leq \tau \sqrt{\frac{2C}{M} \left(\frac{2}{1-\rho} \right)^3}.$$

The proof of Lemma A.15 follows by setting each M_k such that $\rho \cdot d_k + \frac{C}{M_k} = \left(\frac{1+\rho}{2} \right) d_k$, and setting K as the maximal K such that $\sum_{k=1}^K M_k \leq M$. Evaluating $d_K \leq \tau \left(\frac{1+\rho}{2} \right)^K$ yields the result. For convenience, we do not consider burn-in times $M_k \geq M_0 \forall k$ or pseudo-linear dependence $\frac{C \text{polylog}(M_k)}{M_k}$. However, these will only lead to inflating d_K by a $\text{polylog}(M)$ factor.

In essence, Lemma A.15 demonstrates how a fixed offline dataset of size M can be partitioned into independent blocks of increasing size such that the final iterate satisfies an approximate ERM bound scaling as $\frac{1}{\sqrt{M}}$, inflated by a function of the contraction rate ρ . Instantiating Lemma A.15 with the problem parameters of Theorem 3.1 yields Corollary 3.1.

A.4.1 Near-ERM Transfer Learning

An important consequence of Lemma A.15 (thus Corollary 3.1) is that near-ERM parameter recovery bounds can be extracted. In particular, given some $t \in [T + 1]$, for a given representation $\hat{\Phi}$, and the least squares weights $\hat{F}^{(t)}$ computed with respect to some independent dataset of size NT ,

$$\begin{aligned} \left\| \hat{M}^{(t)} - M_\star^{(t)} \right\|_F^2 &= \left\| \hat{F}^{(t)} \hat{\Phi} - F_\star^{(t)} \Phi_\star \right\|_F^2 \\ &= \left\| \hat{F}^{(t)} \hat{\Phi} \begin{bmatrix} \hat{\Phi}^\top & \hat{\Phi}_\perp^\top \end{bmatrix} - F_\star^{(t)} \Phi_\star \begin{bmatrix} \Phi_\star^\top & \Phi_{\star\perp}^\top \end{bmatrix} \right\|_F^2 \\ &= \left\| \begin{bmatrix} \hat{F}^{(t)} - F_\star^{(t)} \Phi_\star \hat{\Phi}^\top & -F_\star^{(t)} \Phi_\star \hat{\Phi}_\perp^\top \end{bmatrix} \right\|_F^2 \\ &= \left\| \hat{F}^{(t)} - F_\star^{(t)} \Phi_\star \hat{\Phi}^\top \right\|_F^2 + \left\| F_\star^{(t)} \Phi_\star \hat{\Phi}_\perp^\top \right\|_F^2 \\ &\leq 2 \left\| F_\star^{(t)} \Phi_\star \left(I_{d_x} - \hat{\Phi}^\top \hat{\Phi} \right) X^{(t)\top} Z^{(t)} \left(\hat{\Sigma}_{z, \mathcal{N}_1}^{(t)} \right)^{-1} \right\|_F^2 \\ &\quad + 2 \left\| W^{(t)\top} Z^{(t)} \left(\hat{\Sigma}_{z, \mathcal{N}_1}^{(t)} \right)^{-1} \right\|_F^2 + \left\| F_\star^{(t)} \right\|_F^2 \text{dist}(\hat{\Phi}, \Phi_\star)^2 \\ &\lesssim \left\| F_\star^{(t)} \right\|_F^2 \kappa \left(\Sigma_x^{(t)} \right) \text{dist}(\hat{\Phi}, \Phi_\star)^2 + \sigma_w^{(t)2} \frac{d_y r + \log(1/\delta)}{\lambda_{\min}(\Sigma_x^{(t)}) NT} \quad \text{w.p.} \geq 1 - \delta, \end{aligned}$$

where the last line follows from applying Lemma A.6. We observe that the parameter error nicely decomposes into a term quadratic in $\text{dist}(\hat{\Phi}, \Phi_\star)$ and least squares fine-tuning error scaling with $\frac{1}{NT}$. For a fixed dataset of size NT , one can crudely set aside $\Theta(N)$ samples for each task, and use the rest of the $\Theta(N)$ samples to compute $\hat{\Phi}$. Invoking Corollary 3.1 and using the set-aside $\Theta(N)$

samples to compute $\hat{F}^{(t)}$ conditioned on $\hat{\Phi}$, we recover the near-ERM high probability generalization bound on the parameter error

$$\left\| \hat{M}^{(t)} - M_{\star}^{(t)} \right\|_F^2 \leq \tilde{O} \left(\left\| F_{\star}^{(t)} \right\|^2 \kappa \left(\Sigma_x^{(t)} \right) C(\rho) \frac{\max_t \sigma_w^{(t)2} d_x r}{NT} + \frac{\sigma_w^{(t)2} d_y r}{\lambda_{\min}(\Sigma_x^{(t)})N} \right).$$

B Case Study: Linear Dynamical Systems

To understand the importance of permitting non-isotropy and sequential dependence in multi-task data, we consider the fundamental setting of linear systems, which has served as a staple testbed for statistical and algorithmic analysis in recent years, since it lends itself to non-trivial yet tractable *continuous* reinforcement learning problems (see e.g., [Fazel et al., 2018, Tu and Recht, 2018, Hu et al., 2023, Krauth et al., 2019, Tu and Recht, 2019, Recht, 2019]), as well as (online) statistical learning problems with temporally dependent covariates [Abbasi-Yadkori et al., 2011, Abbasi-Yadkori, 2013, Simchowitiz and Foster, 2020, Dean et al., 2018, 2020, Agarwal et al., 2019a,b, Ziemann et al., 2022, Ziemann and Sandberg, 2022, Lee et al., 2023, Simchowitiz et al., 2018] (see [Tsiamis et al., 2022] for a tutorial and literature review). In particular for our purposes, the dependence of contiguous covariates in a linear system is intricately connected to its *stability properties* [Simchowitiz et al., 2018, Jedra and Proutiere, 2020, Tu et al., 2022], such that we may instantiate the guarantees of DFW for non-iid data in an interpretable manner.

The standard state-space linear system set-up admits the form

$$\begin{aligned} s[t+1] &= A^{(h)}s[t] + B^{(h)}u[t] + w[t] \\ w[t] &\stackrel{\text{i.i.d.}}{\sim} \mathcal{N}(0, \Sigma_w^{(h)}), \quad s[0] \sim \mathcal{N}(0, \Sigma_0^{(h)}), \end{aligned} \tag{29}$$

where we preemptively index possibly task-specific quantities. We consider the following two common linear system settings: system identification and imitation learning.

B.1 Linear System Identification

In linear system identification, the aim is to estimate the system matrices $(A^{(h)}, B^{(h)})$ given state and input measurements s_t, u_t . In particular, we may cast the sysID problem as the following regression:

$$s[t+1] = \begin{bmatrix} A^{(h)} & B^{(h)} \end{bmatrix} \begin{bmatrix} s[t] \\ u[t] \end{bmatrix} + w[t].$$

It is customary to consider exploratory signals that are iid zero-mean Gaussian random vectors $u[t] \stackrel{\text{i.i.d.}}{\sim} \mathcal{N}(0, \Sigma_u^{(h)})$ [Simchowitiz and Foster, 2020, Simchowitiz et al., 2018, Tsiamis et al., 2022]. In the stable system case, $\rho(A^{(h)}) < 1$, we can therefore evaluate the covariance of the *stationary* distribution of states $s[t]$ induced by exploratory signal $u[t] \stackrel{\text{i.i.d.}}{\sim} \mathcal{N}(0, \Sigma_u^{(h)})$ by plugging in (29) into the following equation

$$\begin{aligned} \mathbb{E}_{u,w}[s[t]s[t]^\top] &= \mathbb{E}_{u,w} \left[s[t+1]s[t+1]^\top \right] \\ &= A^{(h)}\mathbb{E}_{u,w} \left[s[t]s[t]^\top \right] A^{(h)\top} + B^{(h)}\mathbb{E} \left[u[t]u[t]^\top \right] B^{(h)\top} + \mathbb{E} \left[w[t]w[t]^\top \right] \\ &= A^{(h)}\mathbb{E}_{u,w} \left[s[t]s[t]^\top \right] A^{(h)\top} + B^{(h)}\Sigma_u^{(h)}B^{(h)\top} + \Sigma_w^{(h)} \end{aligned}$$

Therefore, evaluating the stationary state covariance $\Sigma_s^{(h)} := \mathbb{E} [s[\infty]s[\infty]^\top]$ amounts to solving the Discrete Lyapunov Equation (`dlyap`):

$$\Sigma_s^{(h)} := A^{(h)}\Sigma_s^{(h)}A^{(h)\top} + B^{(h)}\Sigma_u^{(h)}B^{(h)\top} + \Sigma_w^{(h)}.$$

In the notation introduced earlier in the paper, casting $y[t] \leftarrow s[t+1]$, $x[t] \leftarrow \begin{bmatrix} s[t] \\ u[t] \end{bmatrix}$, $M_\star^{(h)} \leftarrow \begin{bmatrix} A^{(h)} & B^{(h)} \end{bmatrix}$, we may instantiate multi-task linear system identification as a non-iid, non-isotropic linear operator recovery problem.

Definition B.1 *Let the initial state covariance be the stationary covariance $\Sigma_0^{(h)} = \Sigma_s^{(h)}$, such that the covariance of the marginal covariate distribution satisfies*

$$\Sigma_x^{(h)} := \mathbb{E} \left[x[t]x[t]^\top \right] = \begin{bmatrix} \Sigma_s^{(h)} & 0 \\ 0 & \Sigma_u^{(h)} \end{bmatrix}, \text{ for all } t \geq 0.$$

We make the above standard definition for the initial state distribution for convenience, as it ensures the marginal distributions of each state are identical. We note, however, given a different initial state distribution, the marginal state distribution converges exponentially quickly to stationarity, thus accumulating only a negligible factor to the final rates. We then make the following system assumptions to instantiate our representation learning guarantees.

Assumption B.1 *We assume that for any task h the following hold:*

1. *The operators share a rowspace $M_\star^{(h)} := \begin{bmatrix} A^{(h)} & B^{(h)} \end{bmatrix} = F_\star^{(h)}\Phi_\star$, $F_\star^{(h)} \in \mathbb{R}^{d_s \times r}$, $\Phi_\star \in \mathbb{R}^{r \times (d_s + d_u)}$.*
2. *The state matrices have uniformly bounded spectral radii $\rho(A^{(h)}) < \mu < 1$. Subsequently, we assume there exists a constant $\Gamma' > 0$ that satisfies*

$$\|A^{(h)k}\|_2 \leq \Gamma' \mu^k, \text{ for all } k \geq 0.$$

The existence of a uniform Γ' is guaranteed by Gelfand's Formula [Horn and Johnson, 2012], and quantitative bounds may be found in, e.g., Tu and Recht [2018], Goldenshluger and Zeevi [2001].

The first assumption is satisfied, for example, when $A^{(h)} = P_\star^{(h)}U_\star$ and $B^{(h)} = Q_\star^{(h)}V_\star$ individually admit low-rank decompositions. The second assumption translates to a quantitative bound on the mixing time of the covariates $x[t]$ by adapting a result from Tu and Recht [2018].

Proposition B.1 (Adapted from Tu and Recht [2018, Prop. 3.1]) *For each h , let the dynamics for the linear system evolve as described in (29). Let Assumption B.1 hold with constants Γ', ρ . Define $\mathbb{P}_{s[k] \sim \nu_k} [\cdot | s_0 = s]$ as the conditional distribution of states $s[k]$ given initial condition $s_0 = s$. We have for any $k \geq 0$ and initial state distribution ν_0 ,*

$$\mathbb{E}_{s \sim \nu_0} \left[\left\| \mathbb{P}_{s[k]} [\cdot | s_0 = s] - \mathbb{P}_{s[k]} \right\|_{\text{tv}} \right] \leq \frac{\Gamma'}{2} \sqrt{\mathbb{E}_{\nu_0} [\|s[0]\|^2] + \frac{\|\Sigma^{-1}\|_*}{1 - \mu^2}} \cdot \mu^k, \quad (30)$$

where $\|\cdot\|_*$ indicates the nuclear norm [Horn and Johnson, 2012], and $\Sigma := B^{(h)}\Sigma_u^{(h)}B^{(h)\top} + \Sigma_w^{(h)}$.

We note that by the independence of control inputs $u[t]$, we have trivially that the total variation distance between the conditional and marginal distributions of covariates $x[t]$ is the same as that of the states $s[t]$.

$$\left\| \mathbb{P}_{s[k]}[\cdot | s_0 = s] - \mathbb{P}_{s[k]} \right\|_{\text{tv}} = \left\| \mathbb{P}_{x[k]}[\cdot | s_0 = s] - \mathbb{P}_{x[k]} \right\|_{\text{tv}}$$

Since by construction the marginal distribution of states is identically $\mathcal{N}(0, \Sigma_s^{(h)})$, applying Proposition B.1 to $s[t], s[t+k]$ for any t, k , we get the following quantitative bound on the mixing-time of the covariates $x[t] = [s[t]^\top \quad u[t]^\top]^\top$.

Lemma B.1 *Following Definition B.1 and Assumption B.1, the covariate process $\{x^{(h)}[t]\}_{t \geq 0}$ is a mean-zero, stationary, geometrically β -mixing process with covariance $\Sigma_x^{(h)} = \begin{bmatrix} \Sigma_s^{(h)} & 0 \\ 0 & \Sigma_u^{(h)} \end{bmatrix}$, where $\Sigma_s^{(h)} = \text{dlyap}(A^{(h)}, B^{(h)}\Sigma_u^{(h)}B^{(h)} + \Sigma_w^{(h)})$, and mixing-time bounded by*

$$\begin{aligned} \beta(k) &= \Gamma \mu^k, \quad \text{where} \\ \Gamma &:= \frac{\Gamma'}{2} \sqrt{\text{Tr}(\Sigma_s^{(h)}) + \frac{\|\Sigma^{-1}\|_*}{1 - \mu^2}}, \quad \Sigma := B^{(h)}\Sigma_u^{(h)}B^{(h)\top} + \Sigma_w^{(h)}. \end{aligned} \quad (31)$$

Thus, instantiating Lemma B.1 in Theorem A.2 gives us guarantees of DFW applied to multi-task linear system identification.

B.2 Imitation Learning

In linear (state-feedback) imitation learning (IL), the aim is to estimate linear state-feedback controllers $K^{(h)} \in \mathbb{R}^{d_u \times d_x}$ from (noisy) state-input pairs $\{(s[t], u[t])\}_{t \geq 0}$ induced by unknown expert controllers $K_\star^{(h)}$. In particular, we assume the expert control inputs are generated as

$$u[t] = K_\star^{(h)} s[t] + z[t], \quad z[t] \stackrel{\text{i.i.d.}}{\sim} \mathcal{N}(0, \Sigma_z^{(h)}),$$

which we observe lends itself naturally as a linear regression, casting $y[t] \leftarrow u[t]$, $x[t] \leftarrow s[t]$, $M_\star^{(h)} \leftarrow K_\star^{(h)}$. Plugging the expert control inputs into the dynamics (29) yields that the states/covariates evolve as

$$\begin{aligned} s[t+1] &= A^{(h)} s[t] + B^{(h)} \left(K_\star^{(h)} s[t] + z[t] \right) + w[t] \\ &= \left(A^{(h)} + B^{(h)} K_\star^{(h)} \right) s[t] + B z[t] + w[t]. \end{aligned}$$

We make the natural assumption that the expert controller $K_\star^{(h)}$ stabilizes the system, i.e. the spectral radius of the closed-loop dynamics has spectral radius strictly less than 1: $\rho \left(A^{(h)} + B^{(h)} K_\star^{(h)} \right) < 1$. As such, similar to the linear sysID setting, we may plug the above dynamics into the stationarity equation to yield the stationary covariance:

$$\begin{aligned} \mathbb{E}[s[t]s[t]^\top] &= \mathbb{E} \left[s[t+1]s[t+1]^\top \right] \\ &= \left(A^{(h)} + B^{(h)} K_\star^{(h)} \right) \mathbb{E}[s[t]s[t]^\top] \left(A^{(h)} + B^{(h)} K_\star^{(h)} \right)^\top + B^{(h)} \Sigma_z^{(h)} B^{(h)\top} + \Sigma_w^{(h)} \\ \implies \Sigma_s^{(h)} &= \text{dlyap} \left(A^{(h)} + B^{(h)} K_\star^{(h)}, B^{(h)} \Sigma_z^{(h)} B^{(h)\top} + \Sigma_w^{(h)} \right). \end{aligned}$$

Analogously to linear sysID, we make the following assumptions.

Assumption B.2 We assume that for any task h the following hold:

1. The initial state covariance is set to the stationary covariance $\Sigma_0^{(h)} = \Sigma_s^{(h)}$, such that the marginal covariate distributions satisfy

$$\mathbb{E} \left[x[t]x[t]^\top \right] = \Sigma_s^{(h)} =: \Sigma_x^{(h)}, \text{ for all } t \geq 0.$$

2. The controllers share a rowspace $M_\star^{(h)} \equiv K_\star^{(h)} = F_\star^{(t)} \Phi_\star$, $F_\star^{(t)} \in \mathbb{R}^{d_u \times r}$, $\Phi_\star \in \mathbb{R}^{r \times d_s}$.
3. The closed-loop dynamics have uniformly bounded spectral radii $\rho \left(A^{(h)} + B^{(h)} K_\star^{(h)} \right) < \mu < 1$. Subsequently, we assume there exists a constant $\Gamma' > 0$ that satisfies

$$\left\| \left(A^{(h)} + B^{(h)} K_\star^{(h)} \right)^k \right\|_2 \leq \Gamma' \mu^k.$$

The existence of uniform Γ' is guaranteed by Gelfand's Formula [Horn and Johnson, 2012].

By using a result almost identical to Proposition B.1, we yield the following quantitative bound on the mixing time of covariates generated by stabilizing expert controllers.

Lemma B.2 Following Assumption B.2, the covariate process $\{x^{(h)}[t]\}_{t \geq 0}$ is a mean-zero, stationary, geometrically β -mixing process with covariance $\Sigma_x^{(h)} = \Sigma_s^{(h)}$, where $\Sigma_s^{(h)} = \text{dlyap} \left(A^{(h)} + B^{(h)} K_\star^{(h)}, B^{(h)} \Sigma_z^{(h)} B^{(h)\top} + \Sigma_w^{(h)} \right)$, and mixing-time bounded by

$$\beta(k) = \Gamma \mu^k, \text{ where} \quad \Gamma := \frac{\Gamma'}{2} \sqrt{\text{Tr} \left(\Sigma_s^{(h)} \right) + \frac{\|\Sigma^{-1}\|_*}{1 - \mu^2}}, \quad \Sigma := B^{(h)} \Sigma_z^{(h)} B^{(h)\top} + \Sigma_w^{(h)}. \quad (32)$$

Thus, instantiating Lemma B.1 in Theorem A.2 gives us guarantees of DFW applied to multi-task linear imitation learning.

C Additional Numerical Experiments and Details

We present additional numerical experiments to demonstrate the effectiveness of DFW (Algorithm 1) and provide a more detailed explanation of the task-generating process for constructing random operators in linear regression and system identification examples. Furthermore, we introduce an additional setting, imitation learning, to illustrate the advantages of collaborative learning across tasks in learning a linear quadratic regulator by leveraging expert data to compute a shared common representation across all tasks. In this latter setting, we also emphasize the importance of feature whitening when dealing with non-i.i.d. and non-isotropic data.

- **Random rotation:** For all the numerical experiments presented in this paper, the application of a random rotation around the identity is employed for both task-specific weight generation and the initialization of the representation. This random rotation is defined as $R_{\text{rot}} = \exp(\tilde{L})$, where $\tilde{L} = \frac{L - L^\top}{2}$ and $L = \gamma S$. Here, S is a random matrix with entries drawn from a standard normal distribution, d_l is the corresponding dimension of the high-dimensional latent space, and γ corresponds to the scale of the rotation. We set $\gamma = 0.01$ for generating different task weights and $\gamma = 1$ for initializing the representation.

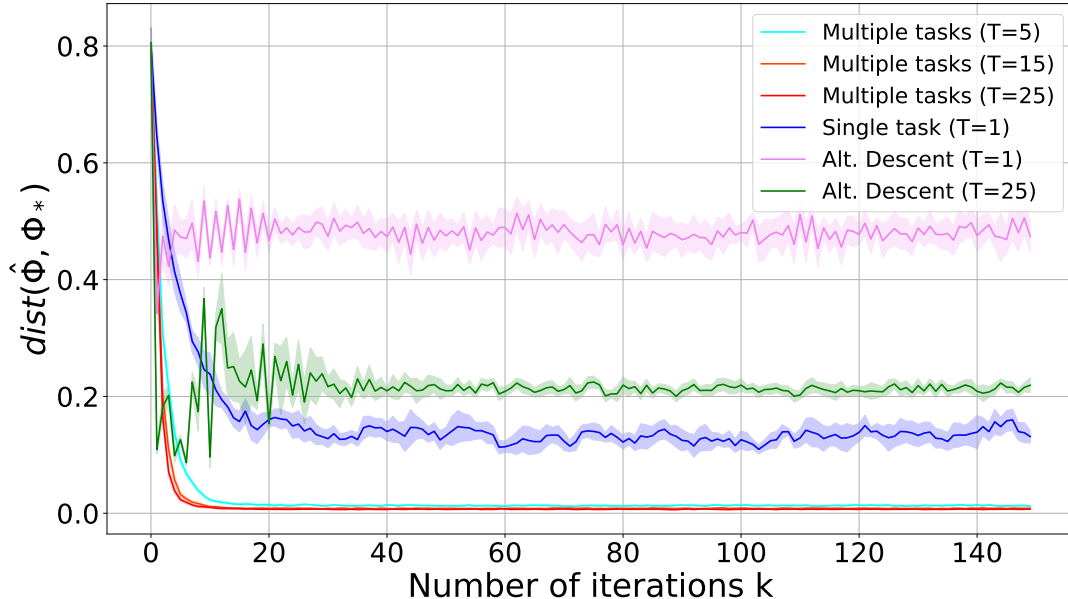


Figure 2: We plot the subspace distance between the current and ground truth representation with respect to the number of iterations, comparing between the single and multiple-task settings of Algorithm 1 and the multi-task FedRep for the IID linear regression with random covariance. We observe performance improvement and variance reduction for multi-task DFW as predicted.

- **Step-sizes:** The step-size η used to update the common representation is carefully selected to ensure a fair comparison between Algorithm 1 and the vanilla alternating minimization-descent approach employed in FedRep Collins et al. [2021]. In Figure 1a, both the single-task and multi-task implementations of Algorithm 1 adopt $\eta = 7.5 \times 10^{-3}$, whereas the vanilla alternating minimization-descent approach uses $\eta = 7.5 \times 10^{-3}$ for a fair comparison. Similarly, in Figure 1c, both the single-task and multi-task versions of Algorithm 1 use $\eta = 1 \times 10^{-1}$, while the vanilla alternating minimization-descent approach utilizes $\eta = 2 \times 10^{-3}$.

C.1 Linear Regression with IID and Non-isotropic Data

Continuing our experiments for the linear regression problem, this time with different random linear operators as illustrated in Figure 1c, we present the results for an extended range of tasks using Algorithm 1 and the alternating minimization-descent approach (FedRep Collins et al. [2021]). In this analysis, we utilize the same specific parameters as discussed in §4. Additionally, we set the step-size $\eta = 7.5 \times 10^{-3}$ for both the single-task and multi-task implementations of Algorithm 1, and $\eta = 7.5 \times 10^{-5}$ for both the single-task and multi-task alternating minimization-descent.

Figure 2 presents a comparison of the performance between Algorithm 1 and the vanilla alternating minimization approach in both single and multi-task settings. In line with our theoretical results, the figure demonstrates that as the number of tasks T increases, the error between the current representation and the ground truth representation significantly diminishes. In the specific case of linear regression with iid and non-isotropic data, this figure emphasizes that a small number of tasks

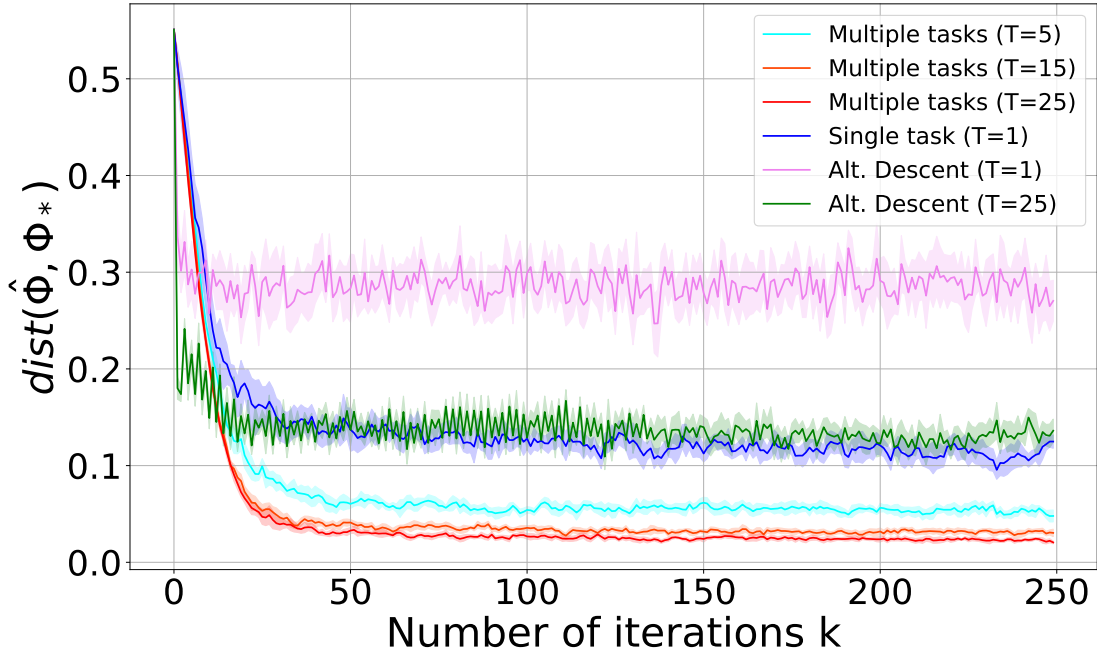


Figure 3: We plot the subspace distance between the current and ground truth representation with respect to the number of iterations, comparing between the single and multiple-task settings of Algorithm 1 multi-task FedRep for the linear system identification with random covariance. We observe performance improvement and variance reduction for multi-task DFW as predicted.

($T = 5$), is sufficient to achieve a low error in computing a shared representation across the tasks. Furthermore, the depicted figure reveals that while the multi-task alternating descent algorithm outperforms the single-task case, it is worth noting that this algorithm remains sub-optimal and is unable to surpass the limitation imposed by the presence of bias in the non-isotropic data. Despite its improved performance, the multi-task alternating descent algorithm still encounters challenges in overcoming the inherent noise barrier.

C.2 System Identification

Building upon the results presented in §4, we conduct an extended experiment involving a larger range of tasks while maintaining the parameters specified in §4.2. Specifically, we generate distinct random operators different from those utilized to obtain the results illustrated in Figure 1c. In this current analysis, we present the outcomes for the expanded range of tasks using Algorithm 1 and compare them to the single-task and multi-task vanilla alternating minimization-descent algorithms. The step-size η is set to 1×10^{-1} for both the single-task and multi-task implementations of Algorithm 1, while for the single-task and multi-task vanilla alternating minimization-descent algorithms, we set η to 2×10^{-3} .

In alignment with our main theoretical findings, Figure 3 provides compelling evidence regarding the advantages of the proposed algorithm (Algorithm 1) compared to the vanilla alternating descent

approach when computing a shared representation for all tasks. Consistent with the trend observed in Figure 2 for the linear regression problem, Figure 3 illustrates a significant reduction in the error between the current representation and the ground truth representation as the number of tasks increases. Additionally, it is noteworthy that while the multi-task alternating descent outperforms the single-task scenario, the single-task variant of Algorithm 1 achieves even better results. This observation underscores the importance of incorporating de-biasing and feature-whitening techniques when dealing with non-iid and non-isotropic data.

C.3 Imitation Learning

Our focus now turns to the problem of learning a linear quadratic regulator (LQR) controller, denoted as $K^{(T+1)} = F_\star^{(T+1)}\Phi_\star$, by imitating the behavior of T expert controllers $K^{(1)}, K^{(2)}, \dots, K^{(T)}$. These controllers share a common low-rank representation and can be decomposed into the form $K^{(t)} = F_\star^{(t)}\Phi_\star$, where $F_\star^{(t)}$ represents the task-specific weight and Φ_\star corresponds to the common representation across all tasks. To achieve this, we exploit Algorithm 1 to compute a shared low-rank representation for all tasks by leveraging data obtained from the expert controllers. Within this context, we consider a discrete-time linear time-invariant dynamical system as follows:

$$x^{(t)}[i+1] = Ax^{(t)}[i] + Bu^{(t)}[i], \quad i = 0, 1, \dots, N-1,$$

with $n_x = 4$ states and $n_u = 4$ inputs, for all $t \in [T+1]$, where $u^{(t)}[i] = K^{(t)}x^{(t)}[i] + z^{(t)}[i]$, with $z^{(t)}[i] \sim \mathcal{N}(0, I_{n_u})$ being the input noise. In our current setting, rather than directly observing the state, we obtain a high-dimensional observation derived from an injective linear function of the state. Specifically, we assume that $y^{(t)}[i] = Gx^{(t)}[i] + w^{(t)}[i]$, where $G \in \mathbb{R}^{25 \times 4}$ represents the high-dimensional linear mapping. The injective linear mapping matrix G is generated by applying a `thin_svd` operation to a random matrix with values drawn from a normal distribution $\mathcal{N}(0, 1)$. This process ensures injectiveness with a high probability.

For this aforementioned multi-task imitation learning setting, we adopt a scheme in which we gather observations of the form $\{\{y^{(t)}[i], u^{(t)}[i]\}_{i=0}^{N-1}\}_{t=1}^T$ from the initial T expert controllers to learn the controller $K^{(T+1)}$. These observations are obtained by following the dynamics:

$$y^{(t)}[i] = (\tilde{A} + \tilde{B}\tilde{K}^{(t)})y[i] + \tilde{B}z^{(t)}[i] + w^{(t)}[i]$$

with $\tilde{A} = GAG^\dagger$, $\tilde{B} = GB$, $\tilde{K}^{(t)} = K^{(t)}G^\dagger$, and process noise $w^{(t)}[i] \sim \mathcal{N}(0, \Sigma_w)$.

The collection of stabilizing LQR controllers $K^{(1)}, K^{(2)}, \dots, K^{(T+1)}$ is generated by assigning different cost matrices, namely $R = \frac{1}{4}I_{n_u}$ and $Q^{(t)} = \alpha^{(t)}I_{n_x}$, where $\alpha^{(t)} \in \text{logspace}(0, 3, H)$. These matrices are then utilized to solve the Discrete Algebraic Ricatti Equation (DARE): $P^{(t)} = A^\top P^{(t)}A^\top + A^\top P^{(t)}B(B^\top P^{(t)}B + R)^{-1}B^\top P^{(t)}A + Q^{(t)}$, and compute $K^{(t)} = -(B^\top P^{(t)}B + R)^{-1}B^\top P^{(t)}A$, for all $t \in [T+1]$. Moreover, the system matrices A and B are randomly generated, with elements drawn from a uniform distribution. The trajectory length $N = 75$ remains consistent for all tasks. The shared representation is initialized by applying a random rotation to the true representation, denoted as $\Phi_\star = G^\dagger$.

Figure 4 presents a comparative analysis between Algorithm 1 and the vanilla alternating minimization-descent approach (**FedRep** in Collins et al. [2021]) for computing a shared representation across linear quadratic regulators. This shared representation is then utilized to derive the learned controller $K^{(T+1)}$ in a few-shot learning manner. Consistent with our theoretical findings and in alignment with the trends observed in Figures 2-3, Figure 4 demonstrates a substantial reduction in the error between the current representation and the ground truth representation when leveraging data from multiple tasks, compared to the single-task scenario in Algorithm 1. Furthermore, this

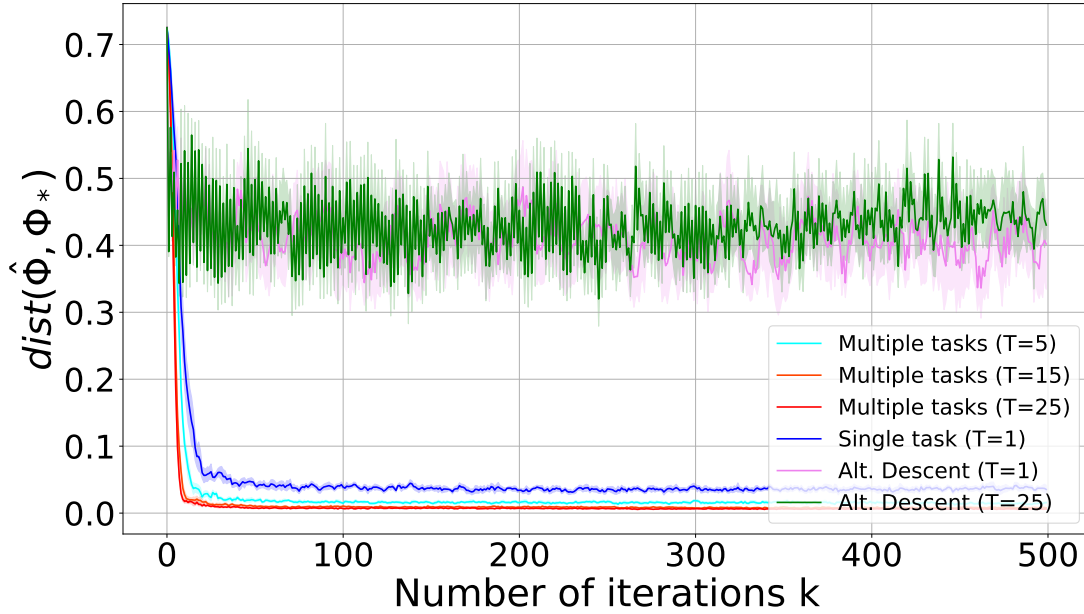


Figure 4: We plot the subspace distance between the current and ground truth representation with respect to the number of iterations, comparing between the single and multiple-task settings of Algorithm 1 and the multi-task FedRep for the imitation learning with random covariance. We observe performance improvement and variance reduction for multi-task DFW as predicted.

figure underscores the significance of de-biasing and whitening the feature data in overcoming the bias barrier introduced by non-iid and non-isotropic data. In contrast, the vanilla alternating descent algorithm fails to address this challenge adequately and yields sub-optimal solutions.